IFM-GEOMAR REPORT

IFM-GEOMAR

Leibniz-Institut für Meereswissenschaften
an der Universität Kiel

FS SONNE
Fahrtbericht / Cruise Report
SO212

Talcahuano, Chile – Valparaiso, Chile
22.12. – 26.12.2010

Berichte aus dem Leibniz-Institut
für Meereswissenschaften an der
Christian-Albrechts-Universität zu Kiel

Nr. 42
Januar 2011

IFM-GEOMAR
Leibniz-Institut für Meereswissenschaften
an der Universität Kiel

FS SONNE
Fahrtbericht / Cruise Report
SO212

Talcahuano - Valparaiso
22.12. – 26.12.2010

Berichte aus dem Leibniz-Institut
für Meereswissenschaften an der
Christian-Albrechts-Universität zu Kiel

Nr. 42
Januar 2011

ISSN Nr.: 1614-6298

IFM-GEOMAR
Leibniz-Institut für Meereswissenschaften
an der Universität Kiel

Das Leibniz-Institut für Meereswissenschaften ist ein Institut der Wissenschaftsgemeinschaft Gottfried Wilhelm Leibniz (WGL)

The Leibniz-Institute of Marine Sciences is a member of the Leibniz Association (Wissenschaftsgemeinschaft Gottfried Wilhelm Leibniz).

Herausgeber / Editor:
Ernst Flüh & Ingo Grevemeyer

IFM-GEOMAR Report
ISSN Nr.: 1614-6298

Leibniz-Institut für Meereswissenschaften / Leibniz Institute of Marine Sciences
IFM-GEOMAR
Dienstgebäude Westufer / West Shore Building
Düsternbrooker Weg 20
D-24105 Kiel
Germany

Leibniz-Institut für Meereswissenschaften / Leibniz Institute of Marine Sciences
IFM-GEOMAR
Dienstgebäude Ostufer / East Shore Building
Wischhofstr. 1-3
D-24148 Kiel
Germany

Tel.: ++49 431 600-0
Fax: ++49 431 600-2805
www.ifm-geomar.de

TABLE OF CONTENTS

1.1 Summary

On February 27, 2010 the second largest earthquake of the 21th century happened in Central Chile. With a magnitude of Mw=8.8 it is among the 5 strongest earthquakes that were instrumentally recorded, and it occurred 50 years after the great 1960 Chile earthquake. It ruptured an area of approx. 800 km length and affected the Chilean provinces Bio-Bio and Maule and thus ruptured the segment to the north of the 1960 rupture zone. In this area, the IFM-GEOMAR and SFB574 had operated an amphibious network of seismological stations for 6 month in 2008, just prior to the earthquake. It was therefore of great interest to observe the aftershocks in this area, so that for the first time a detailed image before and after a megathrust earthquake will be available.

Therefore, during leg SO209-2, from 18. – 21 September 2010 thirty Ocean Bottom Seismometers (OBS) were deployed in the main rupture area between 33° and 36° S.

During leg SO212 from 22. – 26 December 2010, these instruments were recovered, starting from Talcahuano and ending the cruise in Valparaiso. It was possible to quickly check the data quality, and all but one instrument recorded well. Initial results from onboard data analyses exhibit a good data quality and profound results to be expected.

1.2. Zusammenfassung

Am 27. Februar 2010 wurde in Mittelchile das zweitgrößte Erdbeben die Jahrhunderts ausgelöst.Mit einer Magnitude Mw=8.8 gehört es zu den 5 größten Beben, die instrumentell erfasst wurden, und es ereignete sich genau 50 Jahre nach dem großen Chile Beben von 1960. Die Bruchfläche ist ca. 800 km lang und schlisst nach Norden an die Bruchfläche des 1960 Bebens an, die Provinzen Bio-Bio und Maule waren direkt betroffen, In diesem Gebiet wurde vom IFM-GEOMAR und dem SFB574 in Jahre 2008 für sechs Monate ein amphibisches seismologisches Netz betrieben, also unmittelbar vor dem Beben. Es ist daher von besonderem Interesse die Nachbeben auch zu erfassen, so dass es erstmalig möglich ist ein detailliertes Bild der seismogene Zone VOR und NACH einem Großbeben zu erhalten.

Es wurden daher aud der Sonne Fahrt SO209-2 vom 18. – 21. Septemeber 2010 dreizig Ozeanbodenseismometer (OBS) über der Hauptbruchzone zwischen 33° und 36°S ausgebracht. Auf der Ausfahrt SO212 vom 22. – 26.. Dezember 2010 von Talcahuano nach Valparaiso wurde dies wieder geborgen. Eine erste Qualitätskontrolle war an Bord möglich und ergab, dass mit Ausnahme von einem Gerät aller Stationen Daten registriert hatten. Die Daten sind alle von guter Qualität, so dass wichtige neue Ergebnisse erwartet werden können.

1.3 Resumen

El 27 de Febrero del 2010 el segundo terremoto mas grande del siglo 21 sacudió la Zona Central de Chile. Este sismo alcanzó una magnitud de Mw=8.8 y se cuenta entre los 5 terremotos mas grandes que han sido instrumentalmente registrados, y ocurrió 50 años después del gran terremoto de Valdivia en 1960. Este terremoto comprendió a un área de aproximadamente 800 kilómetros de largo afectando las regiones de Maule y Bío-Bío rompiendo un segmento al norte del terremoto de 1960. En esta área y previo al terremoto, IFM-GEOMAR y el proyecto SFB574 instalaron una red sismológica anfibia durante 6 meses en 2008. Es por consiguiente de gran interés observar las replicas en esta área, ya que por primera vez sera posible obtener una imagen sísmica detallada previa y posterior a un mega-terremoto.

Así, durante el crucero SO209-2, llevado a cabo entre el 18 y el 21 de Septiembre del 2010 30 sismómetros de fondo oceánico (OBS) fueron desplegadas en el área de ruptura entre los 33°S y los 36ªS. Durante el crucero SO212, con inicio en Talcahuano y termino en Valparaíso, se realizo entre el 22 y el 26 de Diciembre del 2010, estos instrumentos fueron recuperados. Durante el crucero fue posible hacer una rápida inspección de la calidad de los datos, donde se comprobó que solo uno de los instrumentos no grabo correctamente. Resultados iniciales realizados a bordo dan cuanta de una buena calidad de los datos de los cuales pueden esperarse profundos resultados.

2. Introduction

2.1 Subduction zone earthquakes and co-seismic updip slip termination

Seismologist started recording earthquakes with seismic stations in the early 20th century. In this instrumental record, the 15 largest earthquakes occurred in subduction zones and all magnitude 9 or larger events were subduction thrust megathrust earthquakes. Thus, shallow subduction zone earthquakes present a grave danger to coastal populations from both shaking and from the tsunamis they often generate. Along-strike segmentation controls the length of megathrust ruptures, and thus also has a strong influence on their total magnitude. The amplitude of the tsunami is controlled both by the amplitude of seafloor uplift or subsidence, and whether this occurs in deep or shallow water, which in turn depends on the morphology of the forearc as well as the updip limit of the seismogenic zone.

The updip limit of seaward co-seismic rupture occurs generally not in the trench axis, where both the upper plate (in most cases continental lithosphere) and the subducting lower oceanic plate start sliding along each other, but at greater depth and hence landward of the trench axis. This feature is related to the fact that earthquakes are caused by the frictional properties of the material in the fault zone (Scholz, 1998). It is generally believe that at subduction zones this transition is a temperature-controlled change in sediment mineralogy, especially the dehydration of stable sliding clays. With increasing temperature, smectite clays dehydrate to illite and chlorite, which may exhibit stick-slip or velocity weakening behavior. Most of the transition of smectite to illite and chlorite occurs between 100°C and 150°C (Hyndman and Wang, 1993). However, other processes may affect the transition from velocity strengthening to velocity weakening. Moore and Saffer (2001) show that in accretionary wedges temperatures of 100-150°C correlate with a suit of diagenetic to low-grade metamorphic processes, like active clay, carbonate, and zeolite cementation, the transition to quartz cementation, and declined fluid production and hence decreasing pore pressure. All processes cause an increase in effective stress and strengthening of the hanging wall, which together may cause the onset of velocity weakening during thrust faulting and hence the transition to seismogenic coupling.

The location of the updip limit is particularly important for tsunami generation, as the seaward rupture limit and uplift of seafloor controls tsunami generation

(Pelayo and Wiens, 1992). Based on global data it is generally difficult to define the updip limit. First, slip models from global seismological data generally lack resolution in the trench and slip models are generated introducing predefined rupture areas. The same is the case for geodetic models, as in most subduction zones GPS stations – if they exist – occur only on one side of the subduction zone.

It is, however, possible to assess the rupture area from the distribution of aftershocks (Das and Henry, 2003). However, to make correct associations of earthquakes with tectonic and structural features of an active continental margin it is important to use epicentres that are as accurate as possible. Earthquakes reported in global catalogues have generally been located using automated event locations and often come with large uncertainties. With the obviously complicated structure of a subduction zone and the uneven station distribution contrasting dense coverage on the continent and sparse coverage over the ocean, epicentre bias and inaccuracy are potential issues. Mislocations might be in the order of several tens of kilometres and hence too large defining the seaward updip limit. In Sumatra, a local amphibious seismic network deployed to locate the aftershock activity after the great Sumatra earthquakes of 2004 and 2005 (Tilmann et al., 2010) indicated that events recorded at teleseismic distances had an average mislocation of 17 km, with individual mislocations ranging from 2 to 80 km.

Aftershock locations from a temporary amphibious seismic array in the boundary region between the two large Sumatra earthquakes of 2004 and 2005 indicated that the vast majority of aftershocks occurred on the plate interface within a narrow band (<~20 km). Comparing the seismicity distribution to the co- and post-seismic displacements from global seismic and GPS studies, Tilmann et al. (2010) were able to show that the seismic band marks the transition between the seismogenic zone and stable sliding. Further, the transition zone correlated well with the transition zone of temperatures in the megathrust fault of 100 to 150°C (Grevemeyer and Tiwari, 2006; Tilmann et al., 2010).

2.2 Subduction earthquake cycle and stress transfer from the slab to the other rise

Trench-outer rise earthquakes occur near subduction zones seawards of the trench axis as the oceanic lithosphere approaches a subduction zone and bends into

the deep-sea trench. Plate bending of the incoming lithosphere causes existing faults in the oceanic plate to be reactivated or may create new faults roughly parallel to the trench axis. Chapple and Forsyth (1979) proposed a model in which outer rise earthquakes are a consequence of plate flexure, while the lithosphere is bent into the trench. Their model suggests that the uppermost lithosphere behaves as a thin elastic plate and that downward flexure at the subduction zone leads to a tensional regime at the top of the plate, grading into a compressional regime at the bottom.

However, Christensen and Ruff (1988) proposed that outer rise faulting is sensitive to stress perturbations associated with large underthrusting events in the adjacent subduction zone superimposed on plate bending stresses. When the interplate zone is frictionally locked, the outer rise may experience shallow compressional events, whereas shallow extensional faulting dominates after the megathrust fault ruptures. This interaction may reveal important attributes of the stress state in the subduction zone. Thus, large compressional outer rise faulting earthquakes are generally believed marking subduction zone segments that are locked (Ammon et al., 2008). After a large subduction zone earthquake, the slab pull of the subducted lithosphere is transferred into the other rise, changing its stress state and causing external faulting. This features is best being revealed in the 2006-2007 Kuril island earthquake sequence (Ammon et al., 2008; Lay et al., 2009). On 15 November 2006 a Mw=8.3 subduction zone thrust earthquake ruptured a 250 km long seismic gap. Within minutes of the thrust event, intense earthquake activity commenced beneath the outer wall of the trench seaward of the interplate rupture, with the larger events having normal-faulting mechanisms. An unusual double band of interplate and intraplate aftershocks developed. On 13 January 2007, an Mw = 8.1 extensional earthquake ruptured within the Pacific plate beneath the seaward edge of the Kuril trench.

Stress changes related to the seismic cycle of large interpolate earthquakes may also affect intermediate depth earthquakes. Astiz and Kanamori (1986) studied earthquakes down-dip of the Great 1960 Chile earthquake at 70 to 150 km depth. They observed that events occurring after the interplate earthquake were down-dip compressional while earthquakes occurring before the 1960 earthquake were down-dip tensional. Similar features have been observed elsewhere. Therefore, it seems reasonable to hypothesis that before a major thrust earthquake, the plate boundary is strongly coupled, and the subducted slab is under tension; after the occurrence of an

interpolate thrust event, the displacement on the thrust boundary induces transient compressional stress at intermediate depth in the down-going slab. Thus, both the outer rise and the slab at intermediate depth are affected by temporal variation of stresses due to changes of interplate coupling.

2.3 The Great Chile earthquake of 27 February 2010

The Chilean subduction zone is among the seismic most active fault zones in the world. Most coastal ranges suffered from a magnitude 8 or larger earthquake in the last 150 year, except the Constitución-Concepción segment in Central Chile between ~35.5°S and 37°S, rupturing last in 1835. The area occurs to the north of the nucleation area of the 1960 magnitude 9.5 Valdivia earthquake (37.5°S to 45°S) and to the south of the 1928 magnitude 8 Talca earthquake (~34.5°S to ~35.5°S) (Kelleher, 1972; Beck et al., 1998). The area was considered to be a mature seismic gap, with an expected slip deficit of roughly 10 m (Ruegg et al., 2009). In contrast to other seismic gaps, that just lacks a great magnitude 8 earthquake, was the Constitución-Concepción segment seismically quite without any magnitude 4.5 or larger earthquake reported in global and local catalogues. On 27 February 2010 the seismic quite segment ruptured in a Mw=8.8 earthquake, affecting an area between 33°S and 38.5°S that is roughly three times larger than the seismic gap, including re-rupture of the Talca segment and the nucleation area of the 1960 Valdivia earthquake.

Seismic waves radiated by the mainshock and its largest aftershocks were recorded by hundreds of global broadband seismographs, enabling detailed characterization of the nucleating depth and rupture process. The US Geological Survey (USGS) source parameters (http://earthquake.usgs.gov/regional/world/historical.php) for the earthquake are: 6:34:14.18 UTC, 35.97°S, 72.87°W, Mw=8.8. Waveforms from the mainshock show two features: a roughly 60 s lasting sinus-like waveform superimposed on a 140 s slowly varying ground motion. The first feature is interpreted to be caused by the initial rupture in the nucleation area, while the long-wavelength feature represents bilateral rupture away from the epicentre near the town of Maule, extending roughly 300 km to the south and north, forming a roughly 600 km long fault zone. To study the earthquake, we decomposed the wave field into a 60 s long and 140 s long part

and used a least-squares inversion of azimuthally distributed teleseismic P and SH waveforms, yielding fault geometry and centroid depth of initial rupture (Kikuchi and Kanamori, 1991; Kikuchi and Kanamori, 2004). The initial rupture occurred at 31 +/- 5 km depth near the coast line and had a strike of 30°, a dip of 18°, and a rake of 121°. A nucleation depth of 31 km suggests that the earthquake occurred updip of the continental Moho at 35-40 km (Heit et al., 2008) and hence ruptured a plate contact between subducted sediment and continental crust. The centroid depth of the rupture across the entire fault plain is only poorly resolved, but suggested that slip occurred at <40 km. The fault geometry has a strike of 22°, dip of 17°, and a rake of 121° and thus both compare well with the global CMT (GCMT) solution (strike=18°, dip=18°, rake=112°).

We further computed finite-fault models with prescribed fault orientation, specified rupture velocity Vr, and variable sub-fault rake and source time function. Our preferred solution is for a fault strike of 20° (parallel to coast line), dip of 18°, an average rake of 126°, and Vr=2.6 +/- 0.3 km/s. The seaward limit of slip and the pattern of slip distribution depend strongly on the seaward limit of the prescribed rupture plain. We therefore constrained the seaward extend of rupture by the USGS aftershock distribution, a first-order measure of the location of a rupture area (Das and Henry, 2003). Aftershocks show a well defined distribution, with most aftershocks occurring within a 60-70 wide band between the coastal area and the trench. However, between the trench axis and the aftershock front roughly 40 km landward of the trench virtually no aftershock occur, indicating that frictional properties along the shallow plate boundary support stable sliding instead of seismogenic stick-slip motion (Scholtz, 1998).

The final slip distribution indicates that major slip of >1 m occurred to the north of the Arauco Peninsular, extending from near 37.5°S nearly all the way towards Valpariso at 33°S. The highest slip region of >4 m extended from 37°S offshore of Concepcion to 35.5°S and hence occurs in the area of the 1835 earthquake (Kelleher, 1972; Beck et al., 1998), where approximately 10 m of slip had accumulated since the last earthquake (Ruegg et al., 2008). Slip near Concepcion was between 2 m and 3 m, a value that has been confirmed by GPS measurements that showed that Concepcion slipped by about 3 m southwestward. Re-rupture of the Talca segment caused about 2 m to 3 m of slip between 35.5°S and 34.5°S. Slip within the previously seismic quite patch (Engdahl and Villasenor, 2002) without any

instrumentally recorded seismicity larger than magnitude 4.5 was generally larger than 2 m. Aftershock occurred all the way down to 38.5°S and extended into the nucleation area of the 1960 earthquake, supporting evidence that the Valdivia and Concepcion segments converge at Arauco peninsula (Melnick et al., 2009). However, slip within this region was <1 m. In contrast to the seismically quite gap further north, the area of the Arauco peninsular showed in the past continuous seismic activity (Haberland et al., 2008). Therefore, strain building up in this area is released more continuously over time.

To illuminate processes controlling seaward co-seismic slip termination it might be useful to review the structure of the upper plate and properties of the plate boundary plate using multi-channel seismic data (Cande and Bangs, 1997; Grevemeyer et al., 2003). Continental basement rocks are exposed in the costal cordillera and are interpreted as low-grade metasedimentary rocks that are part of a Paleozoic accretionary wedge and are believed to extend from the coast beyond the edge of the shelf (Scholl et al., 1970; Mordojovich, 1974; Pankhurst et al., 1992). The seismic data indicate a decollement or plate boundary near the toe of the prism at 7.5 s TWT or about 7 km below sea level, dipping at 4-8° and reaching a depth of about 12 km to 14 km below sea level 40 km coastward of the trench near the updip limit of co-seismic rupture. Sediments above have been accreted, forming a 1-2 Mio. years old 15 km to 30 km wide accretionary prism (Bangs and Cande, 1997; von Huene et al., 1997; Grevemeyer et al., 2003) that abuts the continental basement. Therefore, along with the seaward limit of aftershocks occurs a major change in upper plate rheology, with weak and water rich material forming the frontal prism and strong continental basement at the backstop. This change in rheology is supported by seismic refraction and wide-angle data, with seismic velocities <3.5 km/s in the prism and >5 km/s in the continental basement (Contreras-Reyes et al., 2008; Scherwath et al., 2009).

To illuminate processes controlling seaward co-seismic slip termination in the light of the thermal structure, we derive a simple thermal model using analytical solutions derived by Molnar and England (1990). The temperature along the plate boundary reaches 100°C about 20 km landward of the trench, and 150°C roughly 20 km further landward and hence about 40 km coastward of the trench. The updip limit of seismogenic stick-slip behaviour is generally associated with temperatures of 100°C to 150°C. This temperature threshold correlates with a suite of diagentic to

low-grade metamorphic processes, like dehydration of smectite to lillite and chlorite, active clay, carbonate, and zeolite cementation, the transition to quarz cementation, and declined fluid production and hence decreasing pore pressure (Hyndman and Wang, 1993; Moore and Saffer, 2001; Ranero et al., 2008). Thus, in Central Chile two features nurture a velocity strengthening behaviour of rocks at the plate boundary within 20-40 km of the trench axis and velocity weakening and hence seismogenic stick-slip motion further landward. If an earthquake propagates into the stable velocity strengthening region a negative stress drop will occur, resulting in a large energy sink that will rapidly stop the propagation of the earthquake (Scholz, 1998).

A number of aftershocks reported by the USGS occur seaward of the trench in an area where mapping revealed bending-related faulting. A few of the larger earthquakes were reported in the GCMT catalogue, indicating normal faulting and hence may suggest that the slab pull force transferred stress into the outer rise, causing aftershock activity that is not related to stress relaxation along the plate interface. However, a few earthquakes occur in the same setting before the Maule earthquake that may have been bending related. Thus, without local earthquakes recorded in the outer rise the nature of aftershocks (bending-related versus slab pull) is difficult to reveal.

3. Participants

3.1 Scientists - SO 212

Prof. Dr. Ernst R. Flüh	IFM-GEOMAR, chief scientist
Dr. Anke Dannowski	IFM-GEOMAR, SFB 574
Dr. Ivonne Aden-Arroyo	IFM-GEOMAR, SFB 574
Franco Salas Berríos	UV
Juan González-Carrasco	SHOA
Danko Ambrus Perasic	DGF-UCHILE
Maximiliano Leiva Sotomayor	DGF-UCHILE
Geraldine Estay Cubillos	DGF-UCHILE
Jorge Jara Gómez	DGF-UCHILE

3.2 Crew - SO 212

Lutz Mallon	Master
Nils Aden	Chief Mate / 1st Officer
Jens Göbel	2nd Officer
Lars Hoffsommer	2nd Officer
Jörg Leppin	Electronic Engineer
Klaus-Dieter Klinder	Chief Engineer
Sascha Thomsen	2nd Engineer
Uwe Rieper	Electrician
Rainer Rosemeyer	Fitter
Holger Zeitz	Motorman
Torsten Bolik	Motorman
Frank Tiemann	Chief Cook
Andre Garnitz	2nd Cook
Andreas Pohl	Chief Steward
Luis Royo	2nd Steward
Peter Mucke	Boatswain
Jürgen Kraft	A. B.
Ingo Fricke	A. B.
Joachim Dolief	A. B.
Torsten Bierstedt	A. B.
Petra Freiwald	A. B.
Michael Peplow	S.M. / Apprentice
Oliver Eidam	S.M. / Apprentice
Denis Altendorf	S.M. / Apprentice
Steven Ide	S.M. / Apprentice
Andreas Martin	Superintendent
Craig Wallace	Technician

3.3 Addresses of participating institutions

IFM-GEOMAR: Leibniz Institut für Meeresforschung
der Christian-Albrechts-Universität zu Kiel
Wischhofstr. 1-3
24148 Kiel
Germany
Tel.: +49 - 431 - 600 - 2972
Fax: +49 - 431 - 600 - 2922
e-Mail: lname@ifm-geomar.de
Internet: www.ifm-geomar.de

SFB 574: Sonderforschungsbereich an der Christian-Albrechts-Universität zu Kiel
Wischhofstr. 1-3
24148 Kiel
Germany
Tel.: +49 - 431 - 600 - 2972
Fax: +49 - 431 - 600 - 2922
e-Mail: lname@ifm-geomar.de
Internet: www.ifm-geomar.de

SHOA: Servicio Hidrográfico y Oceanográfico de la Armada
Errázuriz 254, Playa Ancha
Valparaíso
Chile
Tel.: +56 - 32 - 226 - 6666
Fax: +56 - 32 - 226 - 6542
e-Mail: jgonzalez@shoa.cl
Internet: www.shoa.mil

DGF-UCHILE: Departamento de Geofísica, Facultad de Ciencias Físicas y Matemáticas, Universidad de Chile
Av. Blanco Encalada 2002, 3° Piso
Santiago
Chile
Tel.: +56 - 2 - 978 - 4562
Fax: +56 - 2 - 696- 8686
e-Mail: lname@dgf.uchile.cl
Internet: www.dgf.uchile.cl

UV: Facultad de Ciencias del Mar, Universidad de Valparaíso
Av. Borgono s/n
Valparaíso
Chile
Tel.: +56 - 32 – 250 - 7820
Fax: +56 - 32 - 250 - 7859
e-Mail: francousteau@yahoo.com
Internet: www.uv.cl

Figure 3.1.1: *Participants of cruise SO212, Talcahuano to Valparaiso.*

4. Agenda

Agenda SO209-2

The RV SONNE leg SO209 was extended by a short second leg to facilitate the deployment of ocean-bottom-seismometers (OBS) in the rupture area of the great Chile earthquake of February 27, 2010. SONNE left the roadstead off Coquimbo on September 17, 2010 at 13:10 local time. After a transit of roughly 24 hours SONNE reached the first deployment position on September 18, 2010 at 12:33 local time and deployed the first OBS at 33°24'S/72°18'W. For the next 2.5 days in total 30 OBS were deployed between 35°40'S and 33°30'S over the continental slope and on the incoming plate; OBS were spaced at roughly 20 sm intervals. On September 20, 2010 at 19:12 local time the last OBS was deployed to the southwest of Valparaíso. After a short transit SONNE reached the pilot station off Valparaíso on September 21, 2010 at 8:00 local time. The locations of the 30 deployed OBS is shown in Figure 4.1.

Members of the scientific party of SO209-2:

Dr. Ingo Grevemeyer
Prof. Dr. Jan Behrmann
Wiebke Brunn
Dr. Eduardo Contreras-Reyes
Claus Hanischdörfer
Stefan Möller
Anne Dörte Rohde
Jochen Schmoll
Dr. Emilio Vera-Somme

r

Figure 4.2: *the science team of SO209-b.*

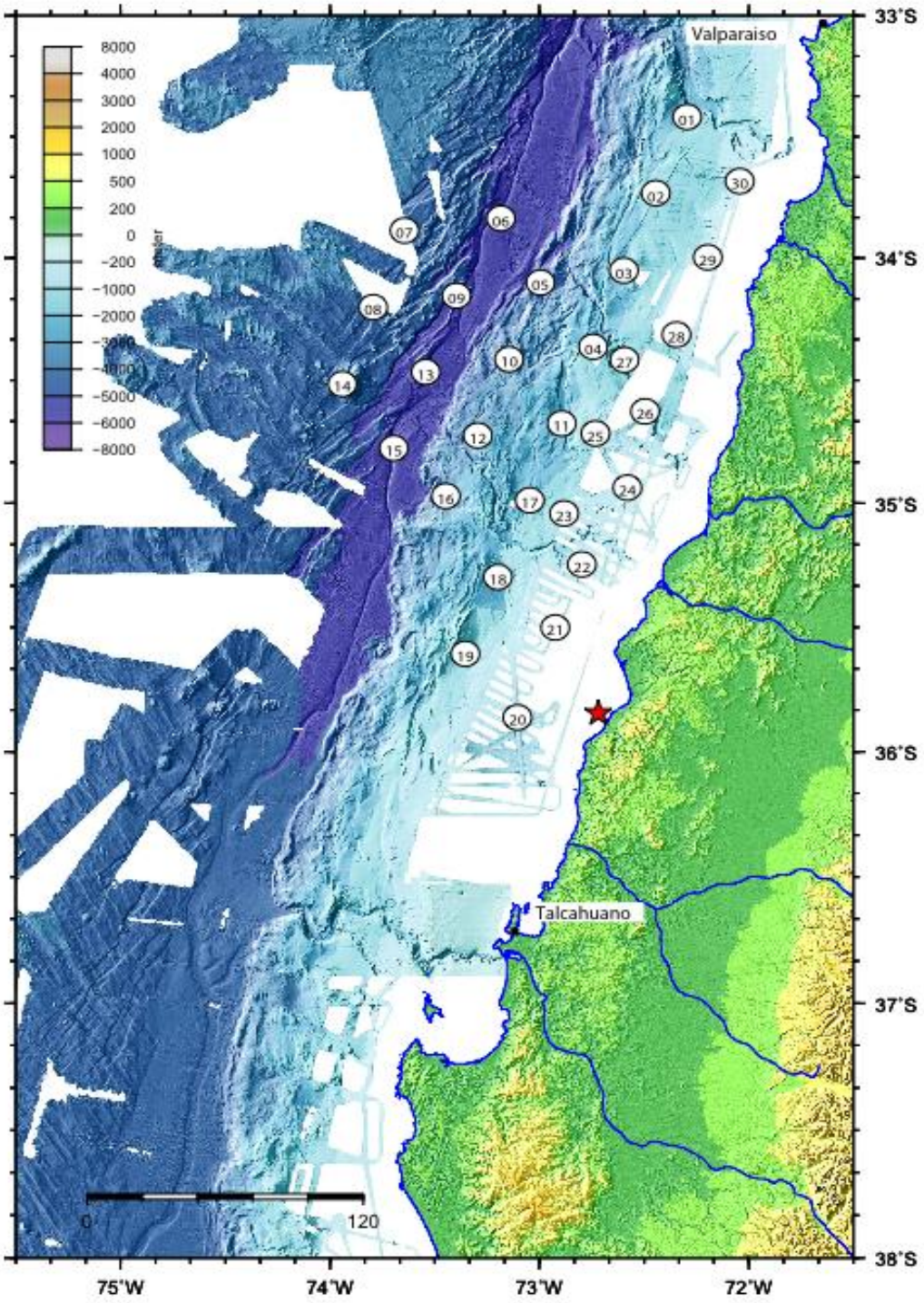

Figure 4.1: *Location map of the instruments deployed. The red star denotes the epicentre of the Maule earthquake*.

Agenda SO212

Cruise SO 212 "TACO" started on December 22 in Talcahuano. Due to severe travel delays of scientists and crew (caused by some snowfall in Europe) and temporal problems in loading scientific equipment and increased administrative paperwork, SONNE could not leave port before 19:30 local time, despite some still missing passengers. The scientific team comprised 9 persons from Chile and Germany.

Right after midnight, the first and southernmost OBS was released and recovered. The multibeam system was started when we had reached a water depth of 200 m outside the 3nm territorial border. After the first OBS we continued northward in a zig-zag line collecting the remaining 29 OBS. The transit speed between stations was favourable (13 nm on average), due to the nicely polished underwater ship's hull. In shallow and moderate water depths instruments were released from a distance such that their surfacing time coincided with the arrival of the vessel. The ascent speed of the OBS is about 1 m/s, so for instruments deployed in deep waters the waiting time sometimes was more than 1 hour. Under favourable conditions, instruments can be released from a distance of up to six miles from their deployment position. We used the hull mounted transducer of SONNE, so release commands could be send at full speed. A total of 11 instruments were recovered on 23.12.

On 24.12, the westernmost instruments, positioned in water depths of up to 5400 m, were recovered first and caused waiting times of more than one hour per station. In total nine instruments were recovered on 24.12. The remaining 10 instruments were all recovered on 25.10 before sunset, and SONNE afterwards continued its travel to the north and reached the planned endpoint, the port of Valparaiso, in the morning of 26.12. At 09:18 local time was at the pier after a journey covering exactly 700 nm.

Weather conditions were favourable throughout the cruise, with only light winds, some sunshine and some fog, and the typical southerly swell, which did however never hinder our work.

In Figure 4.3 a track plot of SO212 is shown.

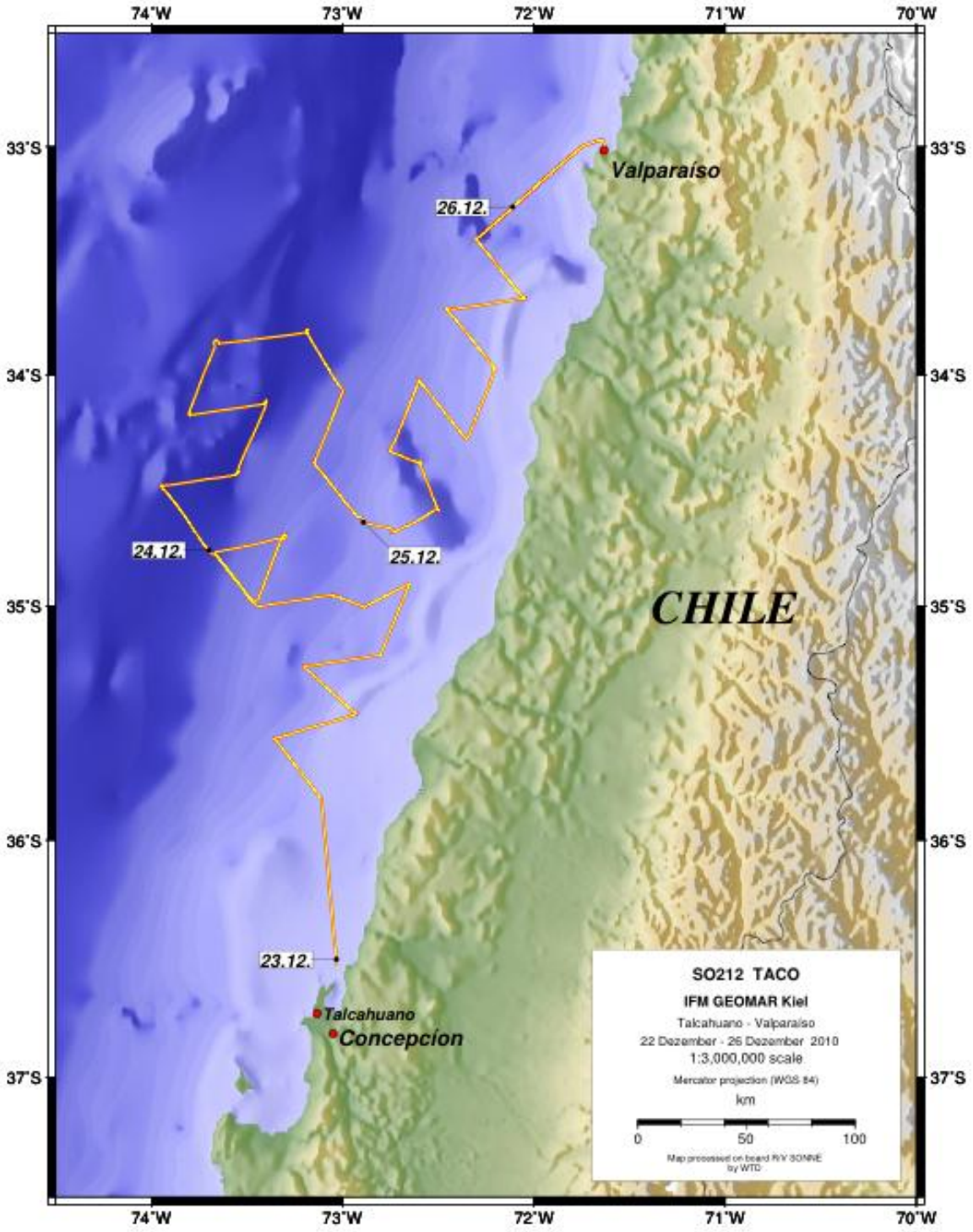

Figure 4.3: *Trackplot of SO212*

5. Scientific equipment

5.1 Shipboard equipment

5.1.1 Navigation

A crucial prerequisite for all kinds of marine surveys is the precise knowledge of position information (latitude, longitude, altitude above/below a reference level). Since 1993 the global positioning system (GPS) is commercially available and widely used for marine surveys. It operates 24 satellites in synchronous orbits, thus at least 3 satellites are visible anywhere at any moment (Seeber, 1996). The full precision of this originally military service yields positioning accuracies of a few meters. In the past this was restricted to military forces and inaccessible to commercial users (Blondel and Murton, 1997). Since about 2000 the full resolution is generally available (with an accuracy in the order of 15 m). During this cruise the operation of the differential (DGPS) option was not requested as standard precision coordinates are precise enough for seismological monitoring stations.

GPS-values as well as most other cruise parameters are continuously stored in the navigation database, and are distributed via the DVS- ("data distribution system") on the ship's network.

5.1.2 Simrad EM120 Swathmapping Bathymetry System

The EM120 system is a multibeam echosounder (with 191 beams) providing accurate bathymetric mapping up to depths higher than 11000 m. This system is composed of two transducer arrays fixed on the hull of the ship, which send successive frequency coded acoustic signals (11.25 to 12.6 kHz). Data acquisition is based on successive emission-reception cycles of this signal. The emission beam is 150° wide across track, and 2° along track direction (Fig. 5.1.2.1). The reception is obtained from 191 overlapping beams, with widths of 2° across track and 20° along it (Fig. 5.1.2.1). The beam spacing can be defined as equidistant or equiangular, and the maximum seafloor coverage fixed or not. The echoes from the intersection area (2°*2°) between transmission and reception patterns (Fig. 5.1.2.1) produce a signal from which depth and reflectivity are extracted.

For depth measurements, 191 isolated depth values are obtained perpendicular to the track for each signal. Using the 2-way-travel-time and the beam angle known for each beam, and taking into account the ray bending due to

refraction in the water column by sound speed variations, depth is estimated for each beam. A combination of phase (for the central beams) and amplitude (lateral beams) is used to provide a measurement accuracy practically independent of the beam pointing angle. The raw depth data need then to be processed to obtain depth-contour maps. In the first step, the data are merged with navigation files to compute their geographic position, and the depth values are plotted on a regular grid to obtain a digital terrain model (*DTM)*. In the last stage, the grid is interpolated, and finally smoothed to obtain a better graphic representation.

Together with depth measurements, the acoustic signal is sampled each 3.2ms and processed to obtain a cartographic representation, commonly named mosaic, where grey levels are representative of backscatter amplitudes. These data provide thus information on the sea-floor nature and texture; it can be simply said that a smooth and soft seabed will backscatter little energy, whereas a rough and hard relief will return a stronger echo.

The EM120 was used continuously during cruise SO212, but occasionally stopped during release attempts of OBS and for maintenance. The data will be processed later and merged with existing data from other cruises.

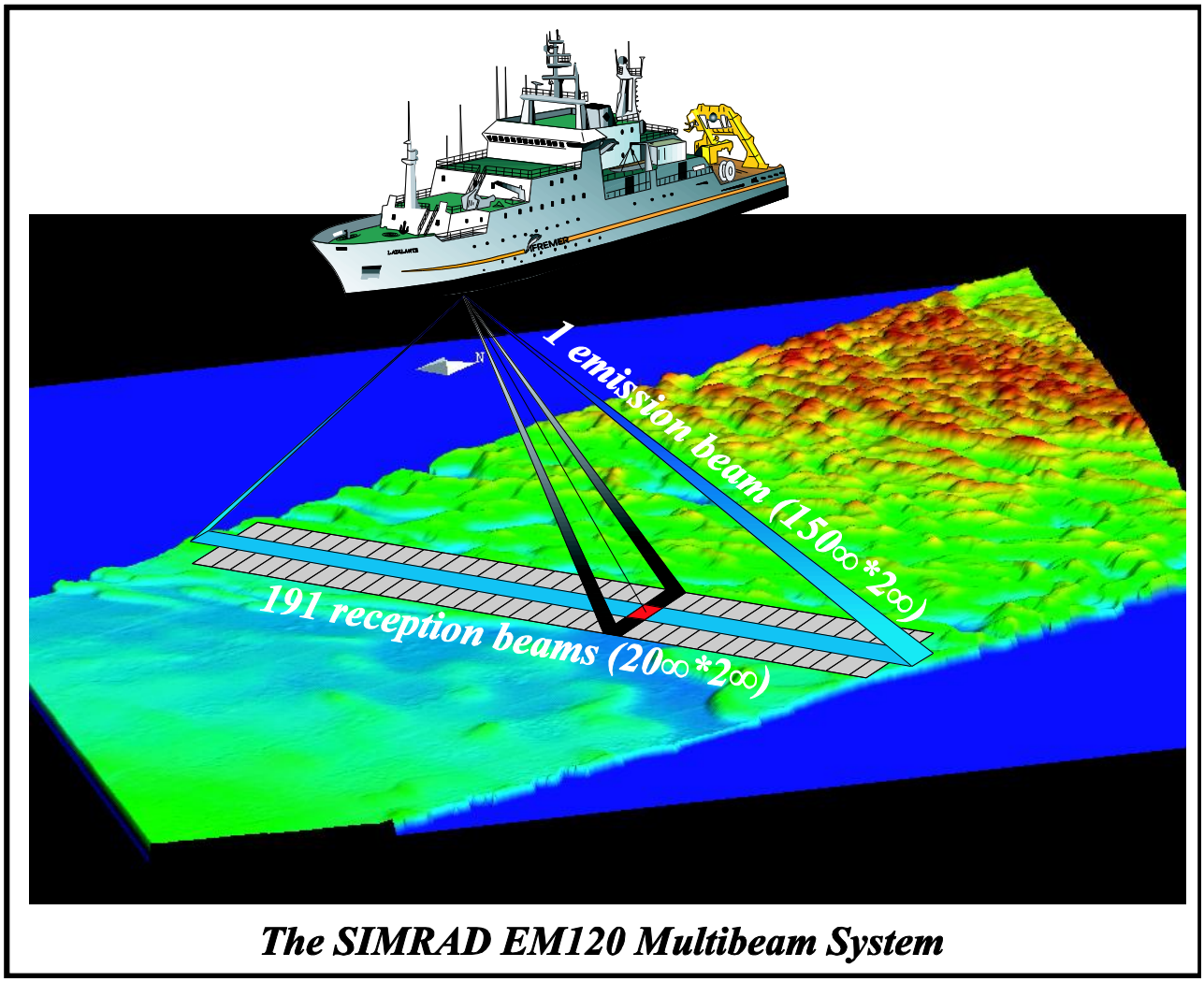

Figure 5.1.2.1: *Acquisition method for bathymetric and backscatter data from the Simrad EM120 system (crossed beams technique).*

5.2 Computer facilities for seismic data processing

The experiment and investigations during SO212 required special computing facilities in addition to the existing shipboard systems. For programming of ocean bottom stations and a first processing of seismic data, a PC-workstation and a dedicated PC-laptop were installed by the working group of IFM-GEOMAR.

The workstation was the following system:

‘caicos”	INTEL Pentium 4 3.2 GHz	2 CPU, 1 GB memory	375 GB disks, 4x PCMCIA	Windows XP Linux (Suse 10.1)

The workstation was placed in the Magnetiklabor. Two Buffalo 500 GB USB-discs were used as backup system. They were ext3 formatted to allow for backup of files larger than 2 GB, typical sizes for seismic data files.

This setup showed a reliable and stable performance, and no breakdowns were observed.

5.3 OBH/OBS seismic instrumentation

The IFM-GEOMAR Ocean Bottom Seismometer 2002

The IFM-GEOMAR Ocean Bottom Seismometer 2002 (OBS-2002) is a design based on experiences gained with the IFM-GEOMAR Ocean Bottom Hydrophone (OBH; Flueh and Bialas, 1996) and the IFM-GEOMAR Ocean Bottom Seismometer (OBS, Bialas and Flueh, 1999). For system compatibility the acoustic release, pressure tubes, and the hydrophones are identical to those used for the OBH. Syntactic foam is used as floatation body again but this time in a less expensive cylinder shape. The entire frame can be dismounted for transportation, which allows storage of more than 50 instruments in one 20” container. Upon cruise preparation onboard all parts are screwed together within a very short time. Four main floatation cylinders are fixed within the system frame, while additional disks can be added to the sides without changes. The basic system is designed to carry a hydrophone and a seismometer. The sensitive seismometer is deployed between the anchor and the OBS frame, which allows good coupling with the sea floor. While the OBS sits on the seafloor, the only connection from the seismometer to the instrument is a cable and an attached wire, which retracts the seismometer during ascent to the sea surface. The three component seismometer (*KUM*) is housed in a titanium tube, modified from a package built by Tim Owen (Cambridge) earlier. Geophones of 4.5 or 15 Hz natural frequency are available. Alternatively, broadband GÜRALP seismometers can be used. The signal of the sensors is recorded by use of the *Marine Longtime Recorder (MLS),* and *Marine Tsunameter Seismocorder (MTS)*, which are manufactured by *SEND GmbH* and specially designed for long-time recordings of

low frequency bands. The hydrophone can be replaced by a differential pressure gauge (DPG) as described by Cox et al (1984).

While deployed to the seafloor the entire system rests horizontally on the anchor frame. After releasing its anchor weight the instrument turns 90° into the vertical and ascends to the surface with the floatation on top. This ensures a maximally reduced system height and water current sensibility at the ground (during measurement). On the other hand the sensors are well protected against damage during recovery and the transponder is kept under water, allowing permanent ranging, while the instrument floats at the surface.

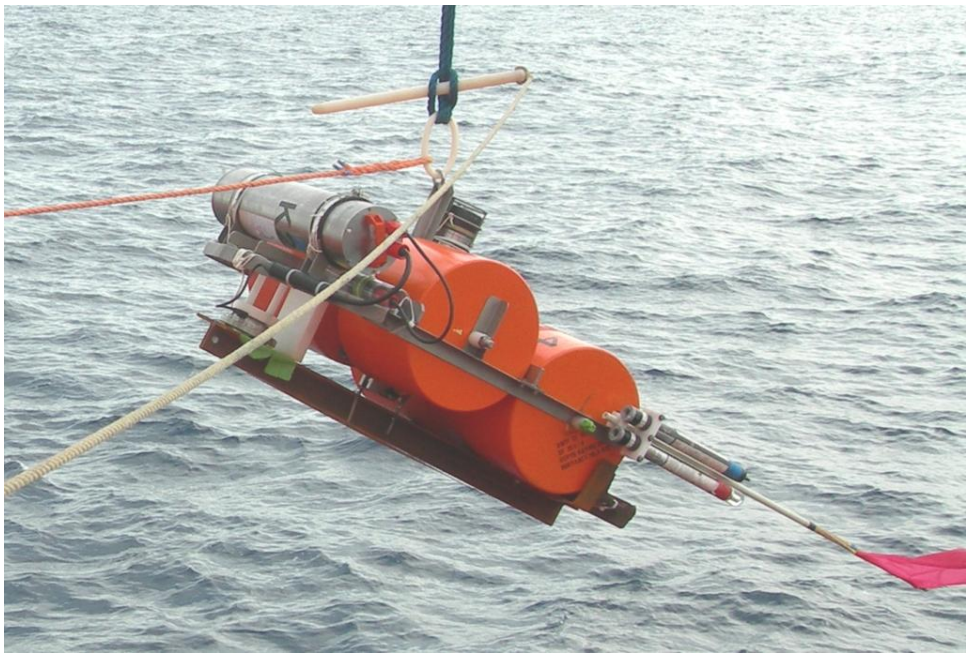

Figure 5.3.1:

OBS 2002, rated for 6000 m.

The IFM-GEOMAR Ocean Bottom Seismometer 8000

The IFM-GEOMAR Ocean Bottom Seismometer 8000 is in principle identical to the OBS2002 described above. However, all components are rated for a maximum deployment depth of 8000 m in contrast to 6000 m for the OBS2002. This implies, since all pressure cylinders are slightly heavier and larger, that additional floatation is required. Also, floatation that is rated for 8000 m has a higher density compared to floatation rated for 6000 m. In summary, the instrument is larger and heavier.

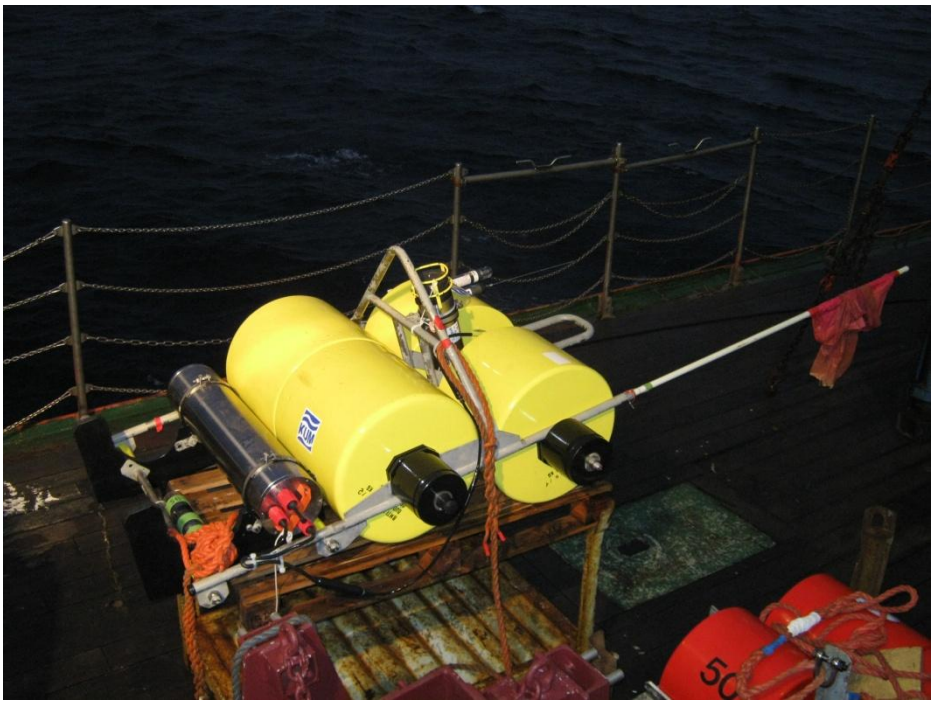

Figure 5.3.2: *OBS 8000, rated for 8000 m depth*

The IFM-GEOMAR Ocean Bottom Marine Longtime Seismograph (MLS)

For the purpose of low-frequency recordings such as seismological observations of earthquakes during long-term deployments of about one year time a data logger, the Marine Longtime Seismograph (MLS) was developed by *SEND GmbH* with support by IFM-GEOMAR.

The MLS is again a four channel data logger whose input channels have been optimised for 3-component seismometers and one hydrophone channel. Due to the modular design of the analogue front end it can be adapted to different seismometers and hydrophones or pressure sensors. Currently front ends for the Spahr Webb, PMD and Güralp seismometers as well as for a differential pressure gauge (DPG), a pressure sensor of high sensitivity and the OAS/HTI hydrophone are available. With these sensors we are able to record events between 50 Hz and 120 s. The very low power consumption of 250 mW during recording together with a high precision internal clock (0.05 ppm drift) allows data acquisition for one year. Data storage is done on up to 12 PCMCIA type II flashcards or microdrives, now available with a capacity of up to 2 GB. The instrument can be parameterised and programmed via a RS232 interface. After low pass filtering the signals of the input

channels are digitised using Sigma-Delta A/D converters. A final decimating sharp digital low-pass filter is realised in software by a Digital Signal Processor. The effective signal resolution depends on the sample rate and varies between 18.5 bit at 20 ms and 22 bits at 1 s. After recording the flashcards need to be copied to a PC workstation. During this transcription the data are decompressed and data files are combined into one data set and formatted according to the PASSCAL data scheme. This enables full compatibility with the established processing system..

The Marine Tsunameter Seismocorder (MTS)

This data logger is based on the experiences with the MBS and MLS devices. The GEOLON-MTS has been developed by *SEND GmbH* and is a high precision instrument for acquisition, processing, storage of seismic signals and additionally pressure data. Like the MLS it is optimised for long time (more than 1 year) standalone operation on the ocean bottom, data storage capacity is also up to 12 PCMCIA cards. The four channel data logger is prepared for connection with a hydrophone (also different types like e.g. HTI, OAS, or the Differential Pressure Gauge, DPG) and different types of three component seismometers as described above for the MLS.

Additionally a digital absolute pressure gauge can be connected to the auxiliary connector, which were used during the deployment at several locations.

Playback of the data is done according to the scheme described for the MLS above. After playback and decompression the data is provided in PASSCAL format.

Figure 5.3.3: *The MLS/MTS seismic recorder.*

6. First Results

Apart from some initial, random visual inspection for data quality, the short time available on board allowed only for a short earthquake location exercise. One of the aftershocks generated during the recording period, according to the catalogues from the USGS and the Servicio Sismológico de Chile (SSC), was cut from the continuous database and located. The event took place on September 30 at 06:27 UTC, and had a magnitude 4.4 ML (SSC). Figure 6.1 shows the vertical component from all the seismometers that recorded the event.

A 1-D velocity model based on a 2-D model (E. Moscoso, pers. comm., 2010) of a wide-angle profile shot in the area in 2008 (Flueh and Bialas, 2008) was used to locate the event. Phase picking and initial location were accomplished using the SEISAN software package (Havskov and Otemoeller, 2008), which includes the program HYP, a modified version of HYPOCENTER (Lienert and Havskov, 1995).

As shown in Figure 6.2, the station coverage for the event is very good (GAP = 138°), with the nearest station located at a distance of 18 km from the hypocenter, which increases the location reliability. The initial location attempted here, including 24 P-wave and 11 S-wave observations, indicates that the earthquake was originated at the outer rise, at a depth of 27 km. The location from the SSC sets the event ~30 km westward, at 31.5 km under the trench (Fig. 6.2). The hypocenter estimated here using the OBS network coincides spatially very well with the outer-rise activity recorded and relocated with the local earthquake tomography technique with data from a passive seismological network deployed in 2008 in the same area (Fig. 6.3). This demonstrates once more the crucial significance of the good ray coverage achieved with ocean-bottom stations for precise earthquake locations at the shallow part of subduction zones, in contrast with locations using only onshore equipment.

Some instruments were also equipped with a Paroscientific depth sensor (see Appendix 9.1), which records the absolute pressure every 15 s. One example of these pressure changes, caused by tides, is shown in Figure 6.4.

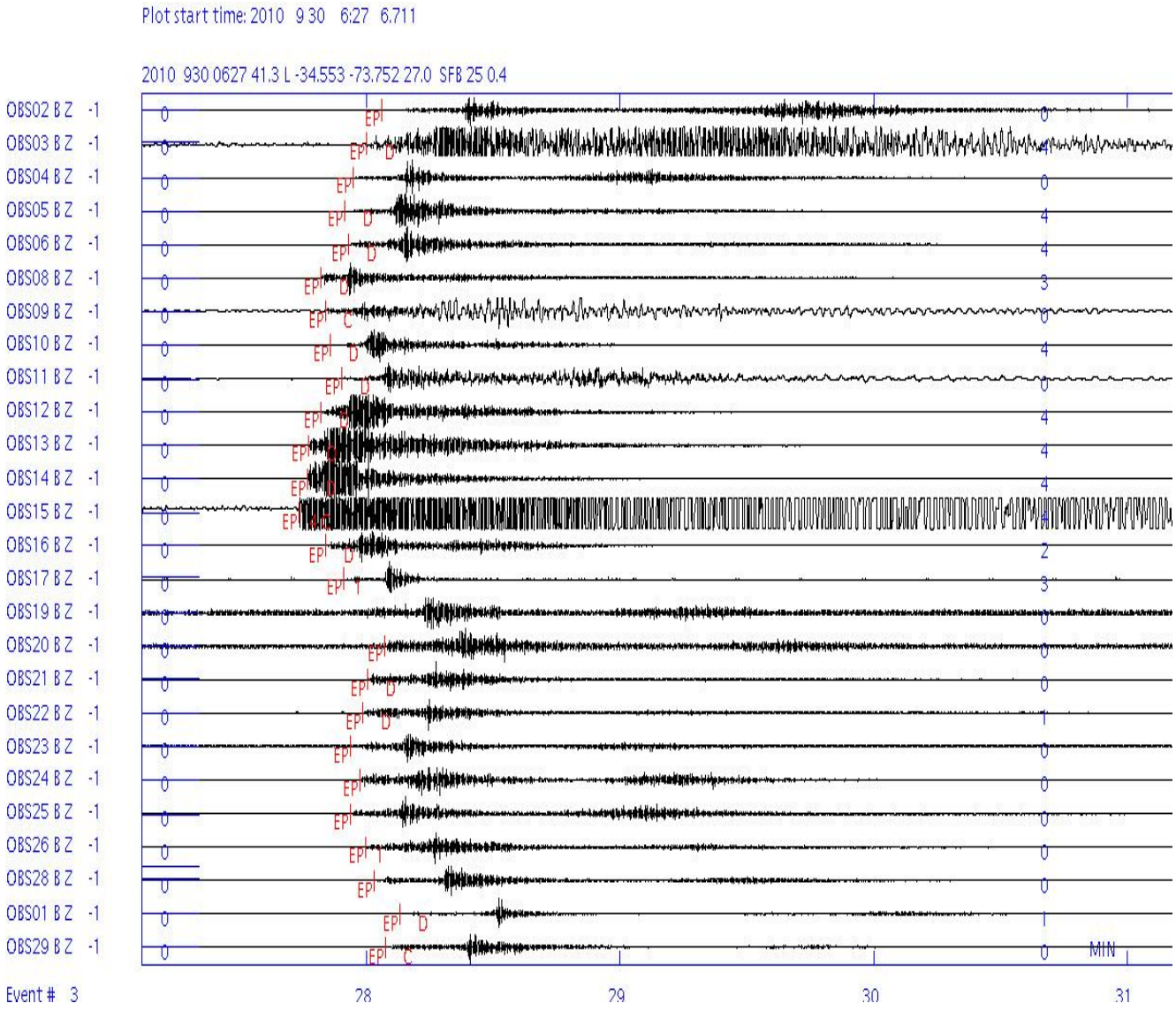

Figure 6.1: *Waveform example. The vertical components of the seismometers are shown for an event generated on September 30 at 06:27 UTC.*

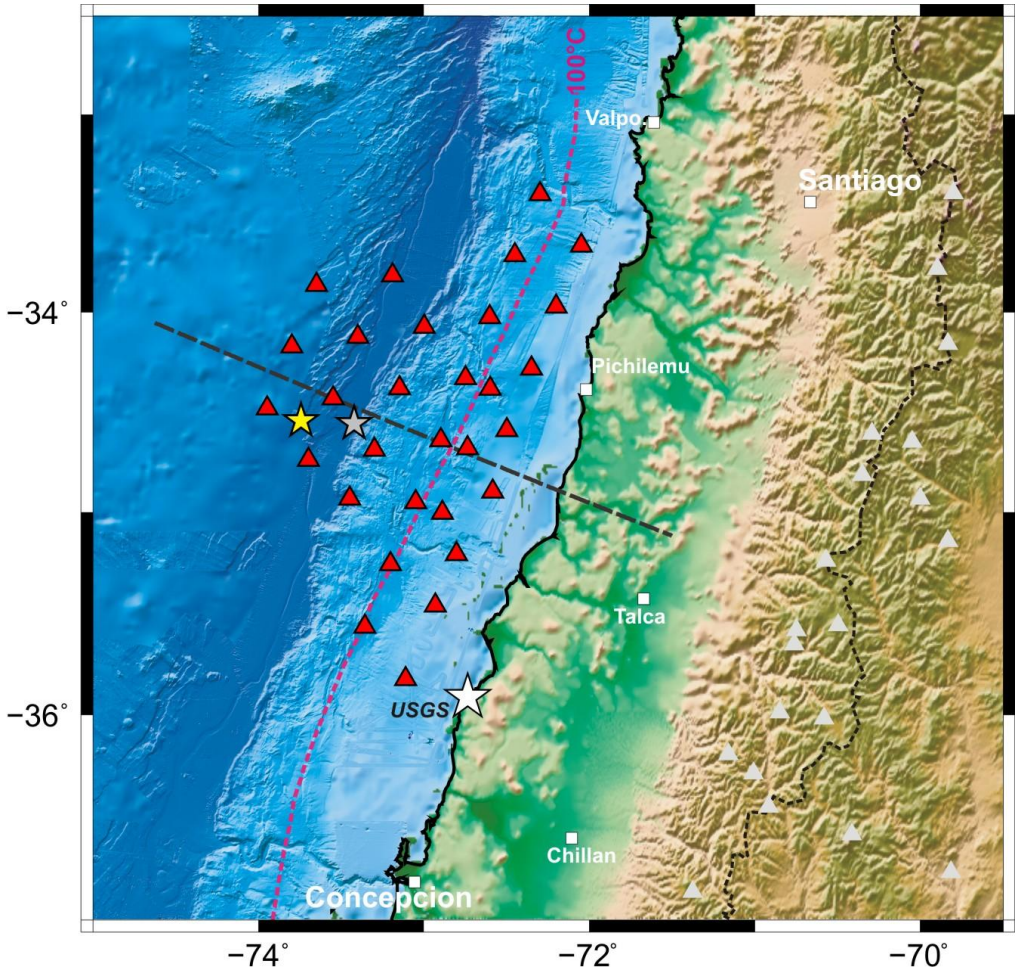

Figure 6.2: *Location of the event generated on September 30 at 06:27 UTC. The yellow star is the epicenter estimated for this report, while the grey star represents the epicenter reported by the Servicio Sismológico de Chile. The dashed line is the orientation of a wide-angle profile shot in 2008, and nearly coincides with the cross-section shown in Figure 6.3. The white star is the rupture start of the Maule Earthquake according to the USGS.*

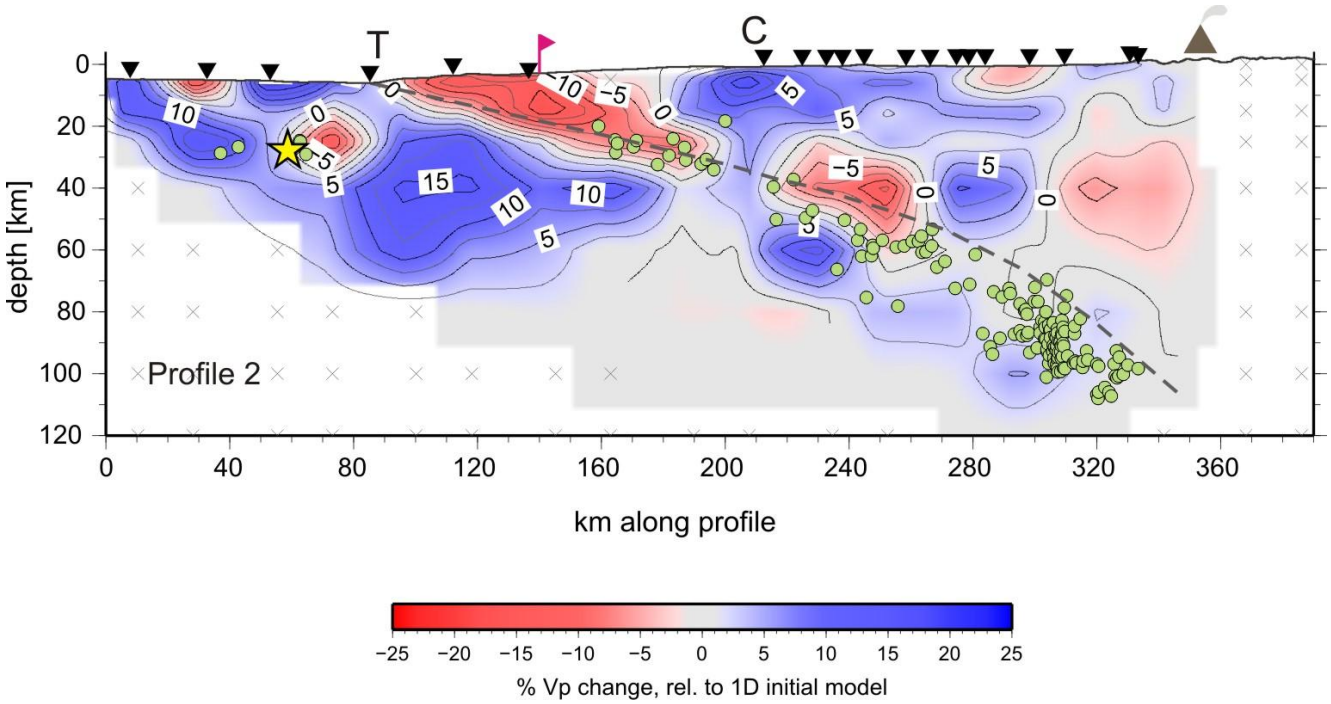

Figure 6.3: *Tomographic section oriented as shown in Figure 6.2. The yellow star is the hypocenter location of the example event located for this report. Observe the good coincidence with the outer-rise activity recorded before the great earthquake. The tomographic model was obtained with data from an 2008 amphibious deployment (I. Arroyo, pers. comm., 2010).*

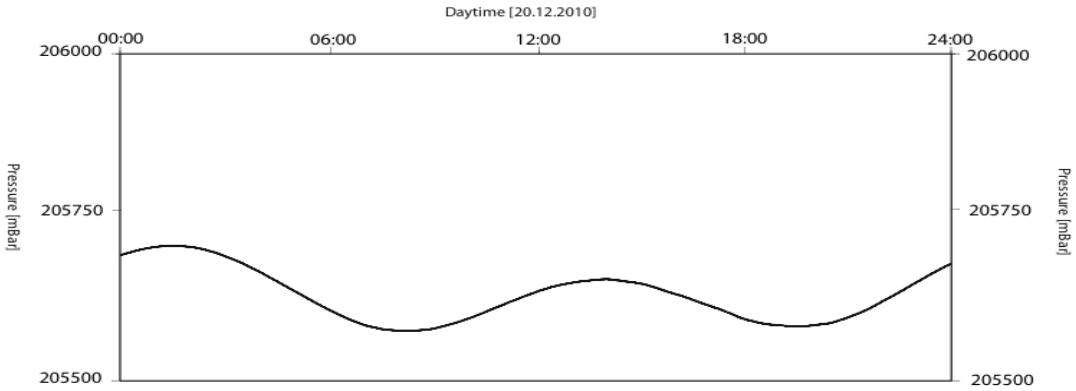

Figure 6.4: *Example of pressure data for 20.12.2010 at station OBS17*

7. Acknowledgement

The cruise SO212 was financed by the German Ministry of Education and Research (BMBF) through grant 03G0212A. We are especially impressed by the ability of BMBF to react promptly to the disasteros Maule earthquake, by providing funds and ship time on short notice. The authors wish to express their gratitude to the various colleagues who have supported the work during the cruise. Particular thanks are directed to the ship's master Captain Lutz Mallon and the crew of RV Sonne.

8. References

Ammon, C.J., Kanamori, H., Lay, T. A great earthquake doublet and seismic stress transfer in the central Kuril islands, *Nature* 451, 561-565, 2008.

Astiz, L., Kanamori, H. Interplate coupling and temporal variation of mechanisms of intermediate-depth earthquakes in Chile, Bull. Seismol.. Soc. Amer. 78, 1614-1622, 1986.

Bangs, N.L., Cande, S.C. Episodic development of a convergent margin inferred from structures and processes along the southern Chile margin, *Tectonics* 16, 489-503, 1997.

Beck, S., Barrientos, S., Kausel, E. ,Reyes, M. Source characteristics of historic earthquakes along the central Chile subduction zone, *J. South Amer. Earth Sci.* 11, 115-129, 1998.

Bialas, J. and Flueh, E. R. Ocean Bottom Seismometers; *Sea Technology*, 40, 4, 41-46, 1999.

Blondel, P., and Muton, B. J. Handbook of seafloor Imagery; John Wiley and Sons, Chichester, pp314, 1997.

Christensen, D. H., Ruff, L. J. Seismic coupling and outer rise earthquakes. J. Geophys. Res. 93, 13421–13444, 1988.

Contreras-Reyes, E., Grevemeyer, I., Flueh, E.R., Reichert, C. Upper lithospheric structure of the subduction zone offshore of southern Arauco Peninsula, Chile at ~38° S, *J. Geophys. Res.* 113, doi:10.1029/2007JB005569, 2008.

Cox, C., Deaton, T., and Webb, S.: A deep-sea differential pressure gauge, J. Atmos. Oceanic Technol., 1(3), 237–246, 1984.

Das, S., Henry C. Spatial relation between main earthquake slip and its aftershock distribution, *Rev. Geophys.* 41, doi:10.1029/2003RG000119, 2003.

Engdahl, E.R., Villasenor, A. Global Seismicity: 1900-1999, *International Handbook of Earthquake and Engineering Seismology* 81A, 665-690, 2002.

Flueh, E. R., and Bialas, J. A digital, high data capacity ocean bottom recorder for seismic investigations; *Int. Underwater Systems Design*, V.18, No. 3, 18-20, 1996.

Flueh, E. R. und Bialas, J., eds. RRS JAMES COOK Fahrtbericht / Cruise Report JC23-A & B : Chile-Margin-Survey, OFEG Barter Cruise with SFB 574 ; 03.03.-25.03. 2008 Valparaiso - Valparaiso ; 26.03.-18.04.2008 Valparaiso - Valparaiso IFM-GEOMAR Report, 20 . IFM-GEOMAR, Kiel, 2008.

Grevemeyer, I., Tiwari, V.M., Overriding plate controls spatial distibution of megathrust earthquakes in the Sunda-Andaman subduction zone, *Earth Planet. Sci. Lett.* 251, 199-208, 2006.

Grevemeyer, I., Diaz-Naveas, J.L., Ranero, C.R., Villinger, H.W., Ocean Drilling Program Leg 202 Scientific Party, Heat flow over the descending Nazca plate in Central Chile, 32°S to 41°S: evidence from ODP Leg 202 and the occurrance of natural gas hydrates, *Earth Planet. Sci. Lett.* 213, 285-298, 2003.

Grevemeyer, I., Kaul, N., Diaz-Naveas, J.C., Villinger, H., Ranero, C.R., Reichert, C. Heat flow and bending-related faulting at subduction trenches: case studies offshore of Nicaragua and Central Chile, *Earth Planet. Sci. Lett.* 236, 238-248, 2005.

Haberland, C., Rietbrock, A., Lange, D., Bataille, K., Dahm T. Structure of the seismogenic zone of the southcentral Chilean margin revealed by local earthquake traveltime tomography, *J. Geophys. Res.* 114, doi:10.1029/2008JB005802, 2009.

Havskov, J., L., and L. Ottemöller, *SEISAN: The Earthquake Analysis Software for Windows, Solaris, LINUX and MACOSX, version 8.2.1*, University of Bergen, Norway, 2008.

Heit, B., Yuan, X., Bianchi, M., Sodoudi, F., Kind, R. Crustal thickness estimation beneath the southern central Andes at 30°S and 36°S from *S* wave receiver function analysis, *Geophys. J. Int.* 174, 249-254, 2008.

Hyndman, R.D., Wang, K. Thermal constraints on the zone of major thrust earthquake failure: the Cascadia subduction zone, *J. Geophys. Res.* 98, 2039-2060, 1993.

Kelleher, J.A. Rupture zones of large south American earthquakes and some predictions, *J. Geophys. Res.* 77, 2087-2103, 1972.

Kikuchi, M., Kanamori H. Inversion of complex body waves-III, Bull. Seism. Soc. Am., 81, 2335-2350, 1991.

Kikuchi M., Kanamori, H. http://www.eri.u-tokyo.ac.jp/ETAL/KIKUCHI, 2004.

Lay, T., Kanamoir, H., Ammon, C.J., Hutko, A.R., Furlong, K., Rivera, L. The 2006-2007 Kuril islands gread earthquake sequence, *J. Geophys. Res.* 114, doi:10.1029/2008JB006280, 2009.

Lienert, B.R.E., and J. Havskov, A computer program for locating earthquakes both locally and globally, *Seism. Res. Lett.*, *66*, 26-36, 1995.

Melnick, D., Bookhagen, B., Strecker M.R. & Echtler H.P.Segmentation of megathrust rupture zones from fore-arc deformation patterns over hundreds to millions of years, Arauco peninsula, Chile, *J. Geophys. Res.* 114, doi:10.1029/2008JB005788, 2009.

Moore, J.C. ,Saffer, D. Updip limit of the seismogenic zone beneath the accretionary prism of southwest Japan: an effect of diagenetic to low-grade metamorphic processes and increasing effective stress, *Geology* 29, 183-186, 2001.

Mordojovich, C. Geology of a part of the Pacific margin of Chile. In: Burk, C.A. & Drake, C.L. (Eds.), pp. 591-598, Springer Verlag, New York, 1974.

Pankhurst, R.J., Hervé, M., Rojas, L., Cembrano, J. Magmatism and tectonics in continental Chiloe, Chile (42°-42°30´S), *Tectonophysics* 205, 283-294, 1992.

Pelayo, A., Wiens, D. Tsunami earthquakes: slow thrust-faulting events in the accretionary wedge, *J. Geophys. Res*., 97, 15321-15337, 1992.

Ranero, C. R., Grevemeyer, I., Sahling, H., Barckhausen, U., Hensen, C., Wallmann, K., Weinrebe, W., Vannucchi, P., von Huene, R., McIntosh, K. Hydrogeological system of erosional convergent margins and its influence on tectonics and interplate seismogenesis, *Geochem. Geophys. Geosyst.* 9, Q03S04, doi:10.1029/2007GC001679, 2008.

Ruegg, J.C., Rudloff, A., Vigny, C., Madariaga, R., de Chabalier, J.B. Campos, J. Kausel, E., Barrientos, S., Dimitrov, D. Interseismic strain accumulation measured by GPS in the seismic gap between Constitución and Concepción in Chile2009, *Phys. Earth Planet. Int.* 175, 78-85, 2009.

Sandwell D., Smith W. H. F., Global marine gravity from Geosat and ERS-1 satellite altimetry, J. Geophys. Res. 102 (1997) 10,039-10,054.

Scherwath, M., Contreras-Reyes, E., Flueh, E.R., Grevemeyer, I., Krabbenhoeft, A., Papenberg, C., Petersen, C.J. ,Weinrebe, W. Deep lithospheric structure along the South Chile margin from wide-angle P-wave modeling, *Geophys. J. Int.* 179, 579-600, 2009.

Scholl, D. W., Christensen, M.N., von Huene, R. ,Marlow, M.S. Peru-Chile trench sediments and seafloor spreading, *Geol. Soc. Am. Bull.* 81, 1339–1360,1970

Scholz, C.H. Earthquakes and friction laws, *Nature* 391, 37-42, 1998.

Seeber, G. Stand und Einsatrzmöglichkeitenvon GPS – ein Überblick; Proc. 11th Annual Meeting of the German Hydrographic Society, Glücksburg, 3.- 5.6.1996.

von Huene, R., et al. Tectonic control of the subducting Juan Fernández Ridge on the Andean margin near Valparaiso, Chile, *Tectonics* 16, 474-488, 1997.

APPENDICES

Appendix 9.1 OBS deployments

	INST.	LAT (S)	LON (W)	DEPLOY.	RECOV.	DEPTH	RELEASER CODE	TIME RELEASE	REC.	Skew	SENSORS
		D:M	D:M	DATE	DATE	(m)		(UTC)	NO.	(ms)	
SO209 – TACO	OBS 01	33:24.357	72:17.988	18.09.10	25.12.10	2073	427737	26.12.10 , 01:00	991234	281	HTI 104, Owen 57
	OBS 02	33:42.876	72:26.968	18.09.10	25.12.10	1608	133477	25.12.10 , 23:00	050817	242	HTI 117, Owen 12, Paro 106112
	OBS 03	34:01.538	72:36.086	18.09.10	25.12.10	2112	533770	25.12.10 , 21:00	040601	005	HTI 85, Güralp T4N61
	OBS 04	34:19.904	72:44.904	18.09.10	25.12.10	2252	646532	25.12.10 , 16:00	991235	213	HTI 51, Owen 33
	OBS 05	34:04.40	72:59.97	19.09.10	24.12.10	4557	646635	25.12.10 , 13:00	991251	-069	HTI 113, Owen 101-121
	OBS 06	33:48.866	73:11.306	19.09.10	24.12.10	5403	534071	25.12.10 , 12:00	010406	108	HTI 109, Owen 112
	OBS 07	33:51.858	73:38.884	19.09.10	24.12.10	4135	534123	25.12.10 , 11:00	991257	no skew	HTI 58, Owen 100-117
	OBS 08	34:10.357	73:47.866	19.09.10	24.12.10	4028	533622	25.12.10 , 10:00	991260	123	HTI 90, Owen 11
	OBS 09	34:07.527	73:23.986	19.09.10	24.12.10	4760	646460	25.12.10 , 14:00	050818	-697	HTI 86, Güralp
	OBS 10	34:22.93	73:08.89	19.09.10	24.12.10	3723	646721	25.12.10 , 15:00	991256	-255	HTI 47, Owen KS1001-120
	OBS 11	34:38.468	72:53.895	19.09.10	25.12.10	2584	534165	25.12.10 , 02:00	050808	245	HTI 57, Güralp T4N26
	OBS 12	34:41.43	73:18.00	19.09.10	23.12.10	3510	430274	25.12.10 , 06:00	081001	251	HTI 73, Owen W01-113
	OBS 13	34:25.946	73:32.895	19.09.10	24.12.10	4960	427623	25.12.10 , 09:00	041104	467	HTI 43, Owen 1001-115, Paro 98612
	OBS 14	34:28.943	73:56.778	19.09.10	24.12.10	3822	133664	25.12.10 , 08:00	991258	768	HTI 87, Owen 1001-114
	OBS 15	34:44.391	73:41.941	19.09.10	24.12.10	5239	133770	25.12.10 , 07:00	010410	-041	HTI 91, Güralp T4N25
	OBS 16	34:55.98	73:26.98	19.09.10	23.12.10	3699	442144	25.12.10 , 05:00	991240	087	HTI 46, Owen 1001-110
	OBS 17	34:57.02	73:02.96	19.09.10	23.12.10	2032	131245	25.12.10 , 03:00	041103	-327	HTI 60, Owen 90, Paro 95933
	OBS 18	35:15.49	73:12.15	20.09.10	23.12.10	2080	534262	25.12.10 , 04:00	040805	no skew	HTI 82, Güralp T4510
	OBS 19	35:34.043	73:21.418	20.09.10	23.12.10	1538	131351	24.12.10 , 20:00	040304	-128	HTI 38, Owen 1001-87
	OBS 20	35:49.475	73:06.653	20.09.10	23.12.10	538	644365	24.12.10 , 16:00	991252	-298	HTI 59, Owen 88
	OBS 21	35:27.765	72:55.820	20.09.10	23.12.10	138	427260	24.12.10 , 21:00	010402	-890	HTI 29, Owen
	OBS 22	35:12.459	72:48.147	20.09.10	23.12.10	670	430135	24.12.10 , 22:00	061201	-268	HTI 107, Owen 89
	OBS 23	35:00.12	72:53.25	20.09.10	23.12.10	1406	134071	24.12.10 , 23:00	040101	-099	HTI 88, Owen 84
	OBS 24	34:53.92	72:35.01	20.09.10	23.12.10	976	430232	25.12.10 , 00:00	081201	-058	HTI 83, Owen KS0403-063
	OBS 25	34:40.88	72:44.23	20.09.10	25.12.10	879	143175	25.12.10 , 01:00	040803	-020	HTI 30 , Owen 0708-099
	OBS 26	34:35.478	72:29.920	20.09.10	25.12.10	1212	646426	25.12.10 , 19:00	000706	332	HTI 32, Owen 1001-118
	OBS 27	34:23.02	72:35.96	20.09.10	25.12.10	1864	646362	25.12.10 , 18:00	050815	498	HTI 20, Güralp T4N21
	OBS 28	34:16.966	72:20.969	20.09.10	25.12.10	743	646276	25.12.10 , 20:00	010408	-185	OAS 46, Owen 0509-073
	OBS 29	33:58.35	72:11.98	20.09.10	25.12.10	689	435445	25.12.10 , 22:00	010403	267	OAS 75, Owen 0509015
	OBS 30	33:39.87	72:02.96	20.09.10	25.12.10	335	134037	26.12.10 , 00:00	991241	216	OAS 07, Owen KS0205-026

Appendix 9.2: Captains Report

Abkürzungen / Abbreviation

z.W	into Water / into water
o.D.	on Deck / on deck
SL (max.)	(maximale)Seillänge / max. rope-length
LT	Lottiefe nach EM 120 / Depth of EM 120
W x	eingesetzte Winde / Winch used
nm	Simrad - Multibeam - Lot / EM 120
PS	Parasound
rwk / COG:	RechtweisEndr Kurs / true course
d:	Distanz / distance
v:	Geschwindigkeit in Knoten / SOG in knots
SL:	Seillänge / rope-length
KL:	Kabellänge / cable-length
SZ:	Seilzug / rope tension

Eingesetzte Geräte / Equiopment used

OBS		fischen	

Einsätze / tasks

30	

Winde	D/M	Type	RF-Nr	SO 212 Tasks	Total tasks	SO 212 length	Total length	Condition	SO 212 max. length	max. rope length ever lowered
W 1	18,2	LWL	110600488	0 h	233 h	0 m	97473 m	3	0 m	3652 m
W 2	18,2	LWL								
W 4	11	Koax	61000273	17 h	60 h	9585 m	23303 m	2	1203 m	2000 m
W 5	11	Koax								
W 6	18,2	Drako	40800193	14 h	855 h	13773 m	790800 m	3	1216 m	7938 m

Station	Date	UTC	PositionLat	PositionLon	Depth [m]	Wind [m/s]	COG [°]	v [kn]	Equipment used	Abbrev.	Action	Remarks
SO212/001-1	23.12.10	03:00	35° 51,11' S	73° 6,49' W	295	SE 1	345	13	OBS/OBH	OBS/OBH	Beginn Station	OBS Fischen
SO212/001-1	23.12.10	03:05	35° 50,11' S	73° 6,63' W	271	NNE 1	353	8	OBS/OBH	OBS/OBH	OBS ausgelöst	OBS 20
SO212/001-1	23.12.10	03:12	35° 49,63' S	73° 6,66' W	265	NE 0	24	2	OBS/OBH	OBS/OBH	OBS gesichtet	OBS 20
SO212/001-1	23.12.10	03:20	35° 49,52' S	73° 6,59' W	265	ENE 2	22	0,5	OBS/OBH	OBS/OBH	OBS an Deck	OBS 20
SO212/001-1	23.12.10	04:47	35° 35,76' S	73° 19,73' W	0	SSE 2	322	12,4	OBS/OBH	OBS/OBH	OBS ausgelöst	OBS 19
SO212/001-1	23.12.10	05:09	35° 34,12' S	73° 21,30' W	0	S 3	307	0,7	OBS/OBH	OBS/OBH	OBS gesichtet	OBS 19
SO212/001-1	23.12.10	05:17	35° 34,08' S	73° 21,49' W	0	SSW 2	248	0,7	OBS/OBH	OBS/OBH	OBS an Deck	OBS 19
SO212/001-1	23.12.10	07:01	35° 27,94' S	72° 56,70' W	144	E 2	70	8,7	OBS/OBH	OBS/OBH	OBS ausgelöst	OBS 21
SO212/001-1	23.12.10	07:03	35° 27,86' S	72° 56,43' W	141	ENE 2	68	6,2	OBS/OBH	OBS/OBH	OBS gesichtet	OBS 21
SO212/001-1	23.12.10	07:12	35° 27,73' S	72° 55,80' W	138	NNE 2	89	0,7	OBS/OBH	OBS/OBH	OBS an Deck	OBS 21
SO212/001-1	23.12.10	08:25	35° 17,57' S	73° 9,36' W	0	SSE 3	308	12,7	OBS/OBH	OBS/OBH	OBS ausgelöst	OBS 18
SO212/001-1	23.12.10	09:04	35° 15,55' S	73° 12,03' W	0	SSE 4	293	0,8	OBS/OBH	OBS/OBH	OBS gesichtet	OBS 18
SO212/001-1	23.12.10	09:16	35° 15,38' S	73° 12,20' W	0	S 5	61	0,6	OBS/OBH	OBS/OBH	OBS an Deck	OBS 18
SO212/001-1	23.12.10	10:41	35° 12,85' S	72° 50,95' W	766	ESE 3	82	13,1	OBS/OBH	OBS/OBH	OBS ausgelöst	OBS 22
SO212/001-1	23.12.10	10:50	35° 12,60' S	72° 48,90' W	702	E 3	81	7	OBS/OBH	OBS/OBH	OBS gesichtet	OBS 22

Geräteverluste / lost Equipment

NIL

SO212/001-1	23.12.10	10:58	35° 12,51' S	72° 48,21' W	661	E 3	87	1,2	OBS/OBH	OBS/OBH	OBS an Deck	OBS 22
SO212/001-1	23.12.10	12:24	34° 55,90' S	72° 39,94' W	924	E 5	19	12	OBS/OBH	OBS/OBH	OBS ausgelöst	OBS 24
SO212/001-1	23.12.10	12:38	34° 54,35' S	72° 39,17' W	1028	ENE 5	37	3,7	OBS/OBH	OBS/OBH	OBS gesichtet	OBS 24
SO212/001-1	23.12.10	12:47	34° 54,03' S	72° 38,99' W	952	E 4	100	1,3	OBS/OBH	OBS/OBH	OBS an Deck	OBS 24
SO212/001-1	23.12.10	13:48	34° 59,28' S	72° 51,31' W	1309	E 4	241	9,8	OBS/OBH	OBS/OBH	OBS ausgelöst	OBS 23
SO212/001-1	23.12.10	14:06	34° 59,99' S	72° 52,90' W	1332	E 5	235	0,8	OBS/OBH	OBS/OBH	OBS gesichtet	OBS 23
SO212/001-1	23.12.10	14:21	35° 0,25 S	72° 53,27' W	1359	ENE 2	320	0,9	OBS/OBH	OBS/OBH	OBS an Deck	OBS 23
SO212/001-1	23.12.10	14:58	34° 57,83' S	73° 0,40' W	1809	ENE 5	292	13,6	OBS/OBH	OBS/OBH	OBS ausgelöst	OBS 17
SO212/001-1	23.12.10	15:26	34° 57,00' S	73° 3,17' W	2012	E 2	72	2,2	OBS/OBH	OBS/OBH	OBS gesichtet	OBS 17
SO212/001-1	23.12.10	15:44	34° 57,06' S	73° 2,92' W	1992	NE 2	300	0,1	OBS/OBH	OBS/OBH	OBS an Deck	OBS 17
SO212/001-1	23.12.10	17:12	34° 59,61' S	73° 23,89' W	3209	SSE 6	259	13	OBS/OBH	OBS/OBH	OBS ausgelöst	OBS 16
SO212/001-1	23.12.10	18:35	34° 47,30' S	73° 39,23' W	4958	SSE 4	316	13,1	OBS/OBH	OBS/OBH	OBS ausgelöst	OBS 15
SO212/001-1	23.12.10	20:07	34° 42,37' S	73° 18,42' W	3451	SSW 6	100	12,3	OBS/OBH	OBS/OBH	OBS ausgelöst	OBS 12
SO212/001-1	23.12.10	20:33	34° 41,41' S	73° 18,01' W	3469	SSW 5	255	1,1	OBS/OBH	OBS/OBH	OBS gesichtet	OBS 12
SO212/001-1	23.12.10	20:44	34° 41,34' S	73° 18,25' W	3538	S 5	327	2,3	OBS/OBH	OBS/OBH	OBS an Deck	OBS 12
SO212/001-1	23.12.10	22:25	34° 58,94' S	73° 27,96' W	4339	SSW 5	248	7,8	OBS/OBH	OBS/OBH	OBS gesichtet	OBS 16
SO212/001-1	23.12.10	22:38	34° 58,51' S	73° 28,83' W	4621	S 7	324	1,5	OBS/OBH	OBS/OBH	OBS an Deck	OBS 16
SO212/001-1	24.12.10	00:07	34° 44,66' S	73° 42,63' W	5230	WSW 6	56	3,4	OBS/OBH	OBS/OBH	OBS gesichtet	OBS 15
SO212/001-1	24.12.10	00:22	34° 45,01' S	73° 42,72' W	5240	SSW 6	267	1,2	OBS/OBH	OBS/OBH	OBS an Deck	OBS 15
SO212/001-1	24.12.10	01:39	34° 32,59' S	73° 53,28' W	3370	S 8	317	12,7	OBS/OBH	OBS/OBH	OBS ausgelöst	OBS 14
SO212/001-1	24.12.10	02:30	34° 28,65' S	73° 57,15' W	3883	SSW 6	92	3,4	OBS/OBH	OBS/OBH	OBS gesichtet	OBS 14
SO212/001-1	24.12.10	02:46	34° 28,90' S	73° 56,67' W	3779	SSW 5	8	0,1	OBS/OBH	OBS/OBH	OBS an Deck	OBS 14
SO212/001-1	24.12.10	04:00	34° 26,83' S	73° 39,74' W	5113	SSW 7	83	12,9	OBS/OBH	OBS/OBH	OBS ausgelöst	OBS 13
SO212/001-1	24.12.10	05:32	34° 25,74' S	73° 32,75' W	4958	SW 7	62	0,2	OBS/OBH	OBS/OBH	OBS gesichtet	OBS 13
SO212/001-1	24.12.10	05:52	34° 25,32' S	73° 32,75' W	4966	SSW 6	289	0,9	OBS/OBH	OBS/OBH	OBS an Deck	OBS 13
SO212/001-1	24.12.10	07:00	34° 12,60' S	73° 26,49' W	5281	SSW 6	21	13,2	OBS/OBH	OBS/OBH	OBS ausgelöst	OBS 09
SO212/001-1	24.12.10	09:15	34° 7,10' S	73° 24,10' W	0	SSW 6	223	2,5	OBS/OBH	OBS/OBH	OBS gesichtet	OBS 09
SO212/001-1	24.12.10	09:22	34° 7,23' S	73° 24,37' W	0	SSW 6	298	0,6	OBS/OBH	OBS/OBH	OBS an Deck	OBS 09
SO212/001-1	24.12.10	10:35	34° 9,71' S	73° 42,19' W	4409	S 4	258	12,7	OBS/OBH	OBS/OBH	OBS ausgelöst	OBS 08
SO212/001-1	24.12.10	11:22	34° 9,94' S	73° 47,96' W	3992	SW 4	13	0,8	OBS/OBH	OBS/OBH	OBS gesichtet	OBS 08
SO212/001-1	24.12.10	11:31	34° 9,94' S	73° 48,00' W	3983	SW 4	276	0,6	OBS/OBH	OBS/OBH	OBS an Deck	OBS 08
SO212/001-1	24.12.10	12:37	33° 57,56' S	73° 42,54' W	4188	S 4	21	13,3	OBS/OBH	OBS/OBH	OBS ausgelöst	OBS 07
SO212/001-1	24.12.10	13:52	33° 51,28' S	73° 39,03' W	4106	SSW 5	159	1,4	OBS/OBH	OBS/OBH	OBS gesichtet	OBS 07
SO212/001-1	24.12.10	14:08	33° 51,64' S	73° 38,95' W	4133	S 5	322	1,7	OBS/OBH	OBS/OBH	OBS an Deck	OBS 07
SO212/001-1	24.12.10	15:35	33° 49,70' S	73° 18,67' W	4810	SSW 8	79	13,6	OBS/OBH	OBS/OBH	OBS ausgelöst	OBS 06
SO212/001-1	24.12.10	16:58	33° 48,17' S	73° 10,90' W	5402	SSW 6	172	1,9	OBS/OBH	OBS/OBH	OBS gesichtet	OBS 06
SO212/001-1	24.12.10	17:06	33° 48,32' S	73° 11,34' W	0	SSW 6	273	1,6	OBS/OBH	OBS/OBH	OBS an Deck	OBS 06
SO212/001-1	24.12.10	18:15	33° 59,14' S	73° 3,82' W	0	SW 10	145	13	OBS/OBH	OBS/OBH	OBS ausgelöst	OBS 05
SO212/001-1	24.12.10	19:20	34° 4,37 S	72° 59,88' W	4521	SW 8	92	0,1	OBS/OBH	OBS/OBH	OBS gesichtet	OBS 05
SO212/001-1	24.12.10	19:27	34° 4,45 S	72° 59,98' W	4549	SSW 8	252	0,5	OBS/OBH	OBS/OBH	OBS an Deck	OBS 05

SO212/001-1	24.12.10	20:37	34° 17,06' S	73° 6,01' W	4093	SW 8	202	12,2	OBS/OBH		OBS/OBH	OBS ausgelöst	OBS 10
SO212/001-1	24.12.10	21:41	34° 22,90' S	73° 8,84' W	4054	SW 8	213	0,2	OBS/OBH		OBS/OBH	OBS gesichtet	OBS 10
SO212/001-1	24.12.10	21:51	34° 22,84' S	73° 8,99' W	3729	SSW 8	334	1,5	OBS/OBH		OBS/OBH	OBS an Deck	OBS 10
SO212/001-1	24.12.10	23:04	34° 34,33' S	72° 57,89' W	2469	SW 13	139	13,1	OBS/OBH		OBS/OBH	OBS ausgelöst	OBS 11
SO212/001-1	25.12.10	00:14	34° 38,34' S	72° 53,63' W	2686	SSW 9	268	4,6	OBS/OBH		OBS/OBH	OBS gesichtet	OBS 11
SO212/001-1	25.12.10	00:30	34° 38,43' S	72° 53,80' W	2573	SSW 10	22	0,6	OBS/OBH		OBS/OBH	OBS an Deck	OBS 11
SO212/001-1	25.12.10	01:08	34° 39,58' S	72° 47,09' W	1341	SSW 12	100	13,1	OBS/OBH		OBS/OBH	OBS ausgelöst	OBS 25
SO212/001-1	25.12.10	01:20	34° 39,97' S	72° 44,65' W	979	SSW 9	92	6,5	OBS/OBH		OBS/OBH	OBS gesichtet	OBS 25
SO212/001-1	25.12.10	01:37	34° 40,87' S	72° 44,17' W	867	SSW 10	76	1	OBS/OBH		OBS/OBH	OBS an Deck	OBS 25
SO212/001-1	25.12.10	02:38	34° 36,08' S	72° 32,80' W	1096	SSW 11	53	12,5	OBS/OBH		OBS/OBH	OBS ausgelöst	OBS 26
SO212/001-1	25.12.10	02:53	34° 34,92' S	72° 30,52' W	1230	SSW 8	84	5,5	OBS/OBH		OBS/OBH	OBS gesichtet	OBS 26
SO212/001-1	25.12.10	03:10	34° 35,28' S	72° 29,95' W	1215	SSW 12	332	0,6	OBS/OBH		OBS/OBH	OBS an Deck	OBS 26
SO212/001-1	25.12.10	04:08	34° 26,02' S	72° 34,33' W	1843	SSW 11	336	13,4	OBS/OBH		OBS/OBH	OBS ausgelöst	OBS 27
SO212/001-1	25.12.10	05:00	34° 22,78' S	72° 35,46' W	1910	SSW 14	170	3,6	OBS/OBH		OBS/OBH	OBS gesichtet	OBS 27
SO212/001-1	25.12.10	05:08	34° 22,96' S	72° 35,59' W	1846	SSW 11	293	1,1	OBS/OBH		OBS/OBH	OBS an Deck	OBS 27
SO212/001-1	25.12.10	06:00	34° 21,53' S	72° 40,47' W	1935	S 14	297	12,5	OBS/OBH		OBS/OBH	OBS ausgelöst	OBS 04
SO212/001-1	25.12.10	06:36	34° 20,28' S	72° 44,11' W	2207	S 13	297	5,3	OBS/OBH		OBS/OBH	OBS gesichtet	OBS 04
SO212/001-1	25.12.10	06:54	34° 19,78' S	72° 45,07' W	2229	S 13	17	1,3	OBS/OBH		OBS/OBH	OBS an Deck	OBS 04
SO212/001-1	25.12.10	08:13	34° 5,79' S	72° 38,01' W	2446	SSW 10	25	13,2	OBS/OBH		OBS/OBH	OBS ausgelöst	OBS 03
SO212/001-1	25.12.10	09:04	34° 1,28' S	72° 35,86' W	2068	SSW 11	191	0,7	OBS/OBH		OBS/OBH	OBS gesichtet	OBS 03
SO212/001-1	25.12.10	09:24	34° 1,39' S	72° 36,20' W	2098	S 9	29	0,5	OBS/OBH		OBS/OBH	OBS an Deck	OBS 03
SO212/001-1	25.12.10	10:58	34° 14,79' S	72° 23,04' W	800	SSW 12	139	11,2	OBS/OBH		OBS/OBH	OBS ausgelöst	OBS 28
SO212/001-1	25.12.10	11:11	34° 16,43' S	72° 21,40' W	754	SSW 11	138	5,9	OBS/OBH		OBS/OBH	OBS gesichtet	OBS 28
SO212/001-1	25.12.10	11:24	34° 16,82' S	72° 21,06' W	748	S 10	268	0,3	OBS/OBH		OBS/OBH	OBS an Deck	OBS 28
SO212/001-1	25.12.10	12:52	34° 0,39' S	72° 13,01' W	490	SSW 11	22	13,6	OBS/OBH		OBS/OBH	OBS ausgelöst	OBS 29
SO212/001-1	25.12.10	13:07	33° 58,28' S	72° 12,16' W	719	W 8	129	4,8	OBS/OBH		OBS/OBH	OBS gesichtet	OBS 29
SO212/001-1	25.12.10	13:16	33° 58,45' S	72° 12,00' W	662	SSW 9	343	1,8	OBS/OBH		OBS/OBH	OBS an Deck	OBS 29
SO212/001-1	25.12.10	14:34	33° 46,06' S	72° 23,94' W	1426	SSW 12	315	13,6	OBS/OBH		OBS/OBH	OBS ausgelöst	OBS 02
SO212/001-1	25.12.10	15:02	33° 42,32' S	72° 27,24' W	1642	W 10	83	4,2	OBS/OBH		OBS/OBH	OBS gesichtet	OBS 02
SO212/001-1	25.12.10	15:15	33° 42,76' S	72° 27,12' W	1613	SW 10	290	1,5	OBS/OBH		OBS/OBH	OBS an Deck	OBS 02
SO212/001-1	25.12.10	16:55	33° 39,99' S	72° 4,03' W	632	SW 8	76	13,8	OBS/OBH		OBS/OBH	OBS ausgelöst	OBS 30
SO212/001-1	25.12.10	17:04	33° 39,69' S	72° 2,50' W	455	WSW 8	184	2,2	OBS/OBH		OBS/OBH	OBS gesichtet	OBS 30
SO212/001-1	25.12.10	17:14	33° 39,84' S	72° 2,93' W	338	SSW 9	5	0,7	OBS/OBH		OBS/OBH	OBS an Deck	OBS 30
SO212/001-1	25.12.10	18:33	33° 27,81' S	72° 14,71' W	1566	SSW 10	321	12,5	OBS/OBH		OBS/OBH	OBS ausgelöst	OBS 01
SO212/001-1	25.12.10	19:03	33° 24,12' S	72° 17,97' W	2070	WSW 8	179	3,2	OBS/OBH		OBS/OBH	OBS gesichtet	OBS 01
SO212/001-1	25.12.10	19:12	33° 24,31' S	72° 17,99' W	2066	WSW 8	311	0,6	OBS/OBH		OBS/OBH	OBS an Deck	OBS 01
SO212/001-1	25.12.10	19:13	33° 24,31' S	72° 17,99' W	2063	SW 8	262	0,2	OBS/OBH		OBS/OBH	Ende Station	

IFM-GEOMAR
Leibniz-Institut für Meereswissenschaften
an der Universität Kiel

IFM-GEOMAR Reports

No.	Title
1	RV Sonne Fahrtbericht / Cruise Report SO 176 & 179 MERAMEX I & II (Merapi Amphibious Experiment) 18.05.-01.06.04 & 16.09.-07.10.04. Ed. by Heidrun Kopp & Ernst R. Flueh, 2004, 206 pp. In English
2	RV Sonne Fahrtbericht / Cruise Report SO 181 TIPTEQ (from The Incoming Plate to mega Thrust EarthQuakes) 06.12.2004.-26.02.2005. Ed. by Ernst R. Flueh & Ingo Grevemeyer, 2005, 533 pp. In English
3	RV Poseidon Fahrtbericht / Cruise Report POS 316 Carbonate Mounds and Aphotic Corals in the NE-Atlantic 03.08.–17.08.2004. Ed. by Olaf Pfannkuche & Christine Utecht, 2005, 64 pp. In English
4	RV Sonne Fahrtbericht / Cruise Report SO 177 - (Sino-German Cooperative Project, South China Sea: Distribution, Formation and Effect of Methane & Gas Hydrate on the Environment) 02.06.-20.07.2004. Ed. by Erwin Suess, Yongyang Huang, Nengyou Wu, Xiqiu Han & Xin Su, 2005, 154 pp. In English and Chinese
5	RV Sonne Fahrtbericht / Cruise Report SO 186 – GITEWS (German Indonesian Tsunami Early Warning System 28.10.-13.1.2005 & 15.11.-28.11.2005 & 07.01.-20.01.2006. Ed. by Ernst R. Flueh, Tilo Schoene & Wilhelm Weinrebe, 2006, 169 pp. In English
6	RV Sonne Fahrtbericht / Cruise Report SO 186 -3 – SeaCause II, 26.02.-16.03.2006. Ed. by Heidrun Kopp & Ernst R. Flueh, 2006, 174 pp. In English
7	RV Meteor, Fahrtbericht / Cruise Report M67/1 CHILE-MARGIN-SURVEY 20.02.-13.03.2006. Ed. by Wilhelm Weinrebe und Silke Schenk, 2006, 112 pp. In English
8	RV Sonne Fahrtbericht / Cruise Report SO 190 - SINDBAD (Seismic and Geoacoustic Investigations Along The Sunda-Banda Arc Transition) 10.11.2006 - 24.12.2006. Ed. by Heidrun Kopp & Ernst R. Flueh, 2006, 193 pp. In English
9	RV Sonne Fahrtbericht / Cruise Report SO 191 - New Vents "Puaretanga Hou" 11.01. - 23.03.2007. Ed. by Jörg Bialas, Jens Greinert, Peter Linke, Olaf Pfannkuche, 2007, 190 pp. In English
10	FS ALKOR Fahrtbericht / Cruise Report AL 275 - Geobiological investigations and sampling of aphotic coral reef ecosystems in the NE-Skagerrak, 24.03. - 30.03.2006, Eds.: Andres Rüggeberg & Armin Form, 39 pp. In English

IFM-GEOMAR
Leibniz-Institut für Meereswissenschaften
an der Universität Kiel

No.	Title
11	FS Sonne / Fahrtbericht / Cruise Report SO 192-1: MANGO: Marine Geoscientific Investigations on the Input and Output of the Kermadec Subduction Zone, 24.03. - 22.04.2007, Ernst Flüh & Heidrun Kopp, 127 pp. In English
12	FS Maria S. Merian / Fahrtbericht / Cruise Report MSM 04-2: Seismic Wide-Angle Profiles, Fort-de-France – Fort-de-France, 03.01. - 19.01.2007, Ed.: Ernst Flüh, 45 pp. In English
13	FS Sonne / Fahrtbericht / Cruise Report SO 193: MANIHIKI Temporal, Spatial, and Tectonic Evolution of Oceanic Plateaus, Suva/Fiji – Apia/Samoa 19.05. - 30.06.2007, Eds.: Reinhard Werner and Folkmar Hauff, 201 pp. In English
14	FS Sonne / Fahrtbericht / Cruise Report SO195: TOTAL TOnga Thrust earthquake Asperity at Louisville Ridge, Suva/Fiji – Suva/Fiji 07.01. - 16.02.2008, Eds.: Ingo Grevemeyer & Ernst R. Flüh, 106 pp. In English
15	RV Poseidon Fahrtbericht / Cruise Report P362-2: West Nile Delta Mud Volcanoes**,** Piräus – Heraklion 09.02. - 25.02.2008, Ed.: Thomas Feseker, 63 pp. In English
16	RV Poseidon Fahrtbericht / Cruise Report P347: Mauritanian Upwelling and Mixing Process Study (MUMP), Las-Palmas - Las Palmas, 18.01. - 05.02.2007, Ed.: Marcus Dengler et al., 34 pp. In English
17	FS Maria S. Merian Fahrtbericht / Cruise Report MSM 04-1: Meridional Overturning Variability Experiment (MOVE 2006), Fort de France – Fort de France, 02.12. – 21.12.2006, Ed.: Thomas J. Müller, 41 pp. In English
18	FS Poseidon Fahrtbericht /Cruise Report P348: SOPRAN: Mauritanian Upwelling Study 2007**,** Las Palmas - Las Palmas**,** 08.02. - 26.02.2007, Ed.: Hermann W. Bange, 42 pp. In English
19	R/V L'ATALANTE Fahrtbericht / Cruise Report IFM-GEOMAR-4: Circulation and Oxygen Distribution in the Tropical Atlantic, Mindelo/Cape Verde - Mindelo/Cape Verde, 23.02. - 15. 03.2008, Ed.: Peter Brandt, 65 pp. In English
20	RRS JAMES COOK Fahrtbericht / Cruise Report JC23-A & B: CHILE-MARGIN-SURVEY, OFEG Barter Cruise with SFB 574, 03.03.-25.03. 2008 Valparaiso – Valparaiso, 26.03.-18.04.2008 Valparaiso - Valparaiso, Eds.: Ernst Flüh & Jörg Bialas, 242 pp. In English
21	FS Poseidon Fahrtbericht / Cruise Report P340 – TYMAS "Tyrrhenische Massivsulfide"**,** Messina – Messina**,** 06.07.-17.07.2006, Eds.: Sven Petersen and Thomas Monecke, 77 pp. In English

IFM-GEOMAR
Leibniz-Institut für Meereswissenschaften
an der Universität Kiel

No.	Title
22	RV Atalante Fahrtbericht / Cruise Report HYDROMAR V (replacement of cruise MSM06/2), Toulon, France - Recife, Brazil, 04.12.2007 - 02.01.2008, Ed.: Sven Petersen, 103 pp. In English
23	RV Atalante Fahrtbericht / Cruise Report MARSUED IV (replacement of MSM06/3), Recife, Brazil - Dakar, Senegal, 07.01. - 31.01.2008, Ed.: Colin Devey, 126 pp. In English
24	RV Poseidon Fahrtbericht / Cruise Report P376 ABYSS Test, Las Palmas - Las Palmas, 10.11. - 03.12.2008, Eds.: Colin Devey and Sven Petersen, 36 pp, In English
25	RV SONNE Fahrtbericht / Cruise Report SO 199 CHRISP Christmas Island Seamount Province and the Investigator Ridge: Age and Causes of Intraplate Volcanism and Geodynamic Evolution of the south-eastern Indian Ocean, Merak/Indonesia – Singapore, 02.08.2008 - 22.09.2008, Eds.: Reinhard Werner, Folkmar Hauff and Kaj Hoernle, 210 pp. In English
26	RV POSEIDON Fahrtbericht / Cruise Report P350: Internal wave and mixing processes studied by contemporaneous hydrographic, current, and seismic measurements, Funchal – Lissabon, 26.04.-10.05.2007 Ed.: Gerd Krahmann, 32 pp. In English
27	RV PELAGIA Fahrtbericht / Cruise Report Cruise 64PE298: West Nile Delta Project Cruise - WND-3, Heraklion - Port Said, 07.11.-25.11.2008, Eds.: Jörg Bialas & Warner Brueckmann, 64 pp. In English
28	FS POSEIDON Fahrtbericht / Cruise Report P379/1: Vulkanismus im Karibik-Kanaren-Korridor (ViKKi), Las Palmas – Mindelo, 25.01.-12.02.2009, Ed.: Svend Duggen, 74 pp. In English
29	FS POSEIDON Fahrtbericht / Cruise Report P379/2: Mid-Atlantic-Researcher Ridge Volcanism (MARRVi), Mindelo- Fort-de-France, 15.02.-08.03.2009, Ed.: Svend Duggen, 80 pp. In English
30	FS METEOR Fahrtbericht / Cruise Report M73/2: Shallow drilling of hydrothermal sites in the Tyrrhenian Sea (PALINDRILL), Genoa – Heraklion, 14.08.2007 – 30.08.2007, Eds.: Sven Petersen & Thomas Monecke, 235 pp. In English
31	FS POSEIDON Fahrtbericht / Cruise Report P388: West Nile Delta Project - WND-4, Valetta – Valetta, 13.07. - 04.08.2009, Eds.: Jörg Bialas & Warner Brückmann, 65 pp. In English
32	FS SONNE Fahrtbericht / Cruise Report SO201-1b: KALMAR (Kurile-Kamchatka and ALeutian MARginal Sea-Island Arc Systems): Geodynamic and Climate Interaction in Space and Time, Yokohama, Japan - Tomakomai, Japan, 10.06. - 06.07.2009, Eds.: Reinhard Werner & Folkmar Hauff, 105 pp. In English
33	FS SONNE Fahrtbericht / Cruise Report SO203: WOODLARK Magma genesis, tectonics and hydrothermalism in the Woodlark Basin, Townsville, Australia - Auckland, New Zealand 27.10. - 06.12.2009, Ed.: Colin Devey, 177 pp. In English

IFM-GEOMAR
Leibniz-Institut für Meereswissenschaften
an der Universität Kiel

No.	Title
34	FS MARIA S. MERIAN Fahrtbericht / Cruise Report MSM 03-2: HYDROMAR IV: The 3rd dimension of the Logatchev hydrothermal field, Fort-de-France - Fort-de-France, 08.11. - 30.11.2006, Ed.: Sven Petersen, 98 pp. In English
35	FS SONNE Fahrtbericht / Cruise Report SO201-2 **KALMAR: K**urile-Kamchatka and **AL**eutian **MAR**ginal Sea-Island Arc Systems: Geodynamic and Climate Interaction in Space and Time Busan/Korea – Tomakomai/Japan, 30.08. - 08.10.2009, Eds.: Wolf-Christian Dullo, Boris Baranov, and Christel van den Bogaard, 233 pp. In English
36	RV CELTIC EXPLORER Fahrtbericht / Cruise Report CE0913: Fluid and gas seepage in the North Sea, Bremerhaven – Bremerhaven 26.07. - 14.08.2009, Eds.: Peter Linke, Mark Schmidt, CE0913 cruise participants, 90 pp. In English
37	FS SONNE Fahrtbericht / Cruise Report: TransBrom SONNE, Tomakomai, Japan - Townsville, Australia, 09.10. - 24.10.2009, Eds.: Birgit Quack & Kirstin Krüger, 84 pp. In English
38	FS POSEIDON Fahrtbericht / Cruise Report POS403, Ponta Delgada (Azores) - Ponta Delgada (Azores), 14.08. - 30.08.2010, Eds.: Torsten Kanzow, Andreas Thurnherr, Klas Lackschewitz, Marcel Rothenbeck, Uwe Koy, Christopher Zappa, Jan Sticklus, Nico Augustin, 66 pp. In English
39	FS SONNE Fahrtbericht/Cruise Report SO208 Leg 1 & 2 Propagation of Galápagos Plume Material in the Equatorial East Pacific (PLUMEFLUX), Caldera/Costa Rica – Guayaquil/Ecuador 15.07. - 29.08.2010, Eds.: Reinhard Werner, Folkmar Hauff and Kaj Hoernle, 230 pp, In English
40	Expedition Report "Glider fleet", Mindelo (São Vincente), Republic of Cape Verde, 05. – 19.03.2010, Ed.: Torsten Kanzow, 26 pp, In English
41	FS SONNE Fahrtbericht / Cruise Report SO206, Caldera, Costa Rica – Caldera, Costa Rica, 30.05. – 19.06.2010, Ed.: Christian Hensen, 95 pp, In English

Das Leibniz-Institut für Meereswissenschaften ist ein Institut der Wissenschaftsgemeinschaft Gottfried Wilhelm Leibniz (WGL)

The Leibniz-Institute of Marine Sciences is a member of the Leibniz Association (Wissenschaftsgemeinschaft Gottfried Wilhelm Leibniz).

Leibniz-Institut für Meereswissenschaften / Leibniz-Institute of Marine Sciences
IFM-GEOMAR
Dienstgebäude Westufer / West Shore Building
Düsternbrooker Weg 20
D-24105 Kiel
Germany

Leibniz-Institut für Meereswissenschaften / Leibniz-Institute of Marine Sciences
IFM-GEOMAR
Dienstgebäude Ostufer / East Shore Building
Wischhofstr. 1-3
D-24148 Kiel
Germany

Tel.: ++49 431 600-0
Fax: ++49 431 600-2805
www.ifm-geomar.de